

## Chapter - 2

### Design of Polygonal Patch and Feed Analysis

#### 2.1. Introduction

As mentioned in chapter 1, patch antennas with different feeds are used in various wireless communication applications. The popular feed types used for patch antenna with comparison are summarized in section 1.2 which are the few reasons why probe feeding is utilized in this work to design the antenna. The key feature of the probe feed which is exploited is the ease of fabrication and its impedance matching. FR-4 material is used as a substrate for the analysis of polygonal patch antennas because it is economic and easily available.

The feed type and position of a polygonal patch antenna plays a vital role for matching the input impedance. The effect of probe feed has been investigated in this chapter with basic polygonal patch antenna geometry i.e. pentagon and hexagon. The effect of probe feed in a non-regular pentagonal patch antenna has been investigated earlier to work in ISM band (Natarajan 2003). A hexagonal shaped patch with probe feed has been reported earlier for a broadband application (Singhal 2005). The variation of the input impedance with feeding position in probe microstrip patch antenna has been investigated. Its analytical calculation to match the input impedance to  $50 \Omega$  transmission line was introduced (Manteghi 2009). Corner truncated probe feed square patch antenna has been investigated for GPS application (Ma 2012). Various algorithms based on Artificial Neural Network, algorithms like Genetic Algorithm have been used for the feed point optimization of probe-fed microstrip antenna (Namkung 2007). To define the objective function for an optimization algorithm that includes all parameters of an antenna for desired performance is still a challenge.

Polygonal patch geometries such as circle, triangle, rectangle, pentagon and hexagon are relatively complicated radiating structure, especially when fed with a probe (Kumar 2002). Bilotti et al. proposed a design of polygonal patch antennas with a broadband behavior by exploiting the electrical antenna features of rectangular patches through proper edge perturbations using full wave analysis (Bilotti 2001) (Bilotti 2003) (Bilotti 2010). Earlier literature suggests that edge perturbation of a rectangular radiator helps in achieving broader bandwidth. The edge perturbation technique can be further explored on circular radiators to study its effect once converted to polygonal geometries. The effect of probe feed (type and position) has been investigated with basic polygonal patch antenna geometry i.e. pentagon and hexagon which show that it plays a significant role in deciding the input impedance (Joshi 2015). Due to ongoing research activity on various polygonal geometries, there is a curious requirement to compare performance of various basic polygon geometries based patch antennas while exploring a suitable probe feed location for justified comparison. Near to accurate simulation software have further motivated for such a study.

Microstrip antennas are popular since decades, but the serious limitations of these antennas has been their narrow bandwidth characteristics. However, it can be improved to certain extent by choosing suitable feeding technique and impedance matching network (Garg 2001). Different geometries of star antenna like four point, five point, etc. are well explored earlier by many researchers, e.g. Abbaspour et al. proposed a wideband and small star-shaped microstrip antenna that has 81% bandwidth over the frequencies 4 to 8.8 GHz with a good cross polarization level and uniform H-plane pattern (Abbaspour 2008).

A star shaped microstrip antenna including a simple feed is proposed by Mirzapour et al. that has a bandwidth of 63% over the frequency range of 5 to 9.3 GHz (Mirzapour 2006). Vertex fed hexagram patch wideband antenna presented wideband of 4 GHz from 7.21 to 11.28 GHz. A star geometry is achieved by moving the midpoint of an edge of polygon

towards center of polygon. As the midpoint moves towards center of polygon exterior angle between vertices of polygon reduces. The effect of geometry perturbation of polygon to polygram on antenna characteristics is observed, evaluated and presented, in this chapter. A basic polygonal patch antenna e.g., a pentagonal patch reflects wideband characteristics as analyzed earlier (Joshi 2014) and presented with a hexagonal patch antenna for the purpose of comparison with polygram antenna designs after edge perturbations.

Various gain improvement techniques such as EBG, fractals, stacked patches, slot loaded patches, slit loaded patches can be applied to microstrip antennas with rectangular, circular or triangular patches have been reviewed (Siakavara 2011).

A patch with metallic ring causes the enhancement in the gain as well as impedance bandwidth as compared to patch without metallic ring has been presented by kumar et al. It was observed that gain is enhanced by 4.3 dB and impedance bandwidth is enhanced by 2 percent when patch is surrounded by metallic ring as compared to the patch without metallic ring. Analysis of the fields in the substrate shows that surface wave are scattered from metallic ring and convert into the space waves (Kumar 2014). Zhang et al. designed, built and analyzed a wideband, high-gain, circularly polarized antenna combined with coaxial balun feed. The antenna has good impedance characteristic, symmetrical radiation patterns in both principal planes, low back radiation, wide axial-ratio bandwidth, and good gain performance (Zhang 2013).

Comparing both pentagonal and hexagonal designs, it was observed that pentagonal patch permits better gain than hexagonal patch over the band of 11.4 to 20 GHz (Joshi 2015). Even polygon to polygram can improve gain of an antenna. The effect of edge perturbation in polygonal patch antenna design is studied. Pentagon or pentagram geometries provide a wider bandwidth than hexagon or hexagram geometries. No significant variation is observed in antenna characteristics when polygons are transformed to polygram geometries, other than

a slight improvement in gain of the hexagon patch when transformed to hexagram geometry with  $\theta = 163.15^\circ$  (Joshi 2015). So, there is requirement to analyse polygonal slot in polygonal patch antenna to improve gain.

In this chapter the basics required for understanding the polygonal patch antenna and its characteristics are discussed. The effect of probe feed i.e. location of the probe on various characteristics such as impedance and gain of polygonal patch antenna especially a pentagon and hexagon are examined and analyzed in section 2.2. In section 2.3, various polygonal geometries such as triangle, rectangle, pentagon, hexagon and circle are used to design a L-band probe fed radiator and performance are compared to analyse its characteristics. The advantages and disadvantages of various radiators are also discussed with its fundamental phenomenon of radiation. The similar comparison and analysis of various polygonal geometries as analyzed in section 2.3 is done in the X-band by designing X-band quarter wave radiator in section 2.4 of the chapter. Various issues associated with the different polygonal radiator are also discussed. How the characteristics of the antenna is changes when the edges of the polygonal radiator is perturbed is discussed in section 2.5 of the paper. The pros and cons associated with the edge perturbation of pentagon and hexagon are investigated in detail. Finally in section 2.6, a polygonal slot technique to enhance the gain of vertex fed polygonal patch antenna at higher frequencies are presented.

This chapter explicitly presents the properties, features and issues of polygonal patch and edge perturbation by changing the original structure with probe feed on FR-4 substrate through simulations only.

## **2.2. Probe Feed Effect in Polygonal Patch Antennas**

A regular pentagonal patch antenna is designed in CST MWS as shown in Figure 2.1. The regular pentagon geometry applied here, has a distance of 27 mm from center of pentagon to

vertex of pentagon. This antenna is designed on a glass epoxy FR-4 substrate ( $\epsilon_r = 4.3$ ,  $\tan \delta = 0.025$ , substrate thickness = 1.5 mm). The regular pentagon patch has (X-Y) dimensions of 54 mm  $\times$  94 mm. The substrate has dimensions of 80 mm  $\times$  80 mm and the ground plane has an area of 60 mm  $\times$  52.6 mm as shown in Figure 2.1. The center of the ground plane and regular pentagon patch coincides and both conducting layers have the same thickness of 0.035 mm.

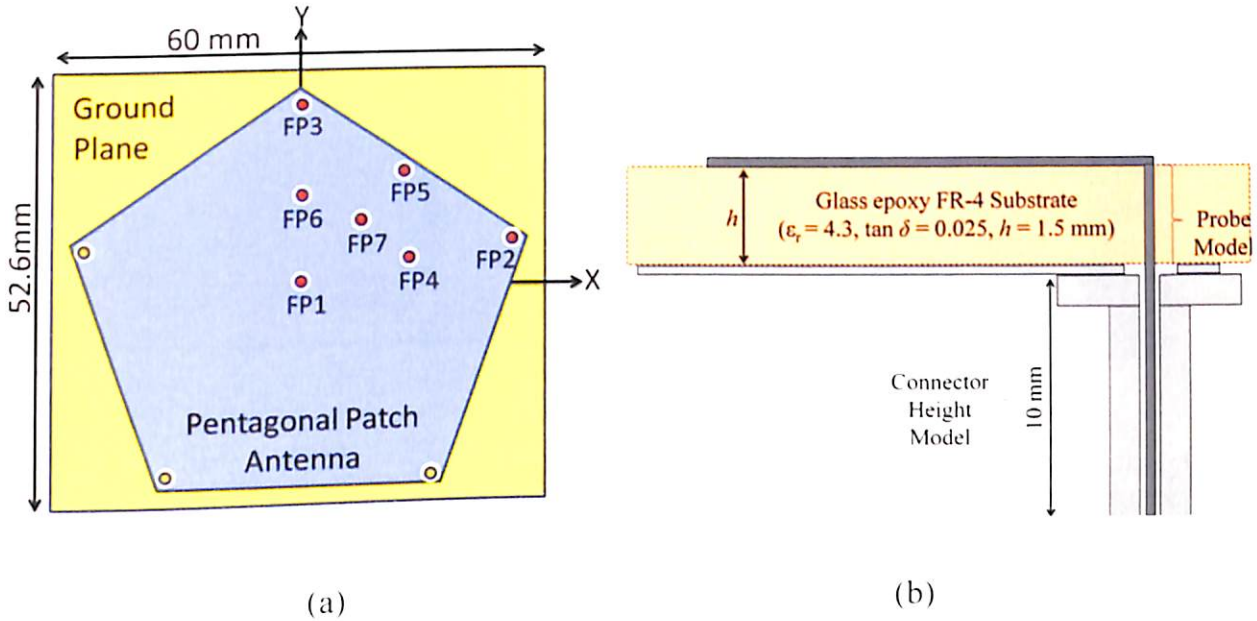


**Figure 2.1.** (a) Geometry of the proposed pentagonal-shaped patch antenna with the feed points indicated (b) Side view.

The antenna is fed through a probe feed arrangement by using a standard SMA connector. All vertices of polygonal patch are connected to SMA indicated by yellow (light) color points in Figure 2.1 but it is observed during simulations that the presence of feed points indicated by yellow (light) color points do not have significant effect on the performance of the antenna. Feed points (FP1 to FP7) indicated by red (dark) color points are excited one at a time through direct coaxial probe-feed to demonstrate the effect of probe feed in pentagonal-shaped patch antenna.

Similarly, a regular hexagonal patch antenna with feed points (FP1 to FP7) is designed with a distance of 27 mm from center to vertex of the hexagonal patch as shown in Figure 2.2.

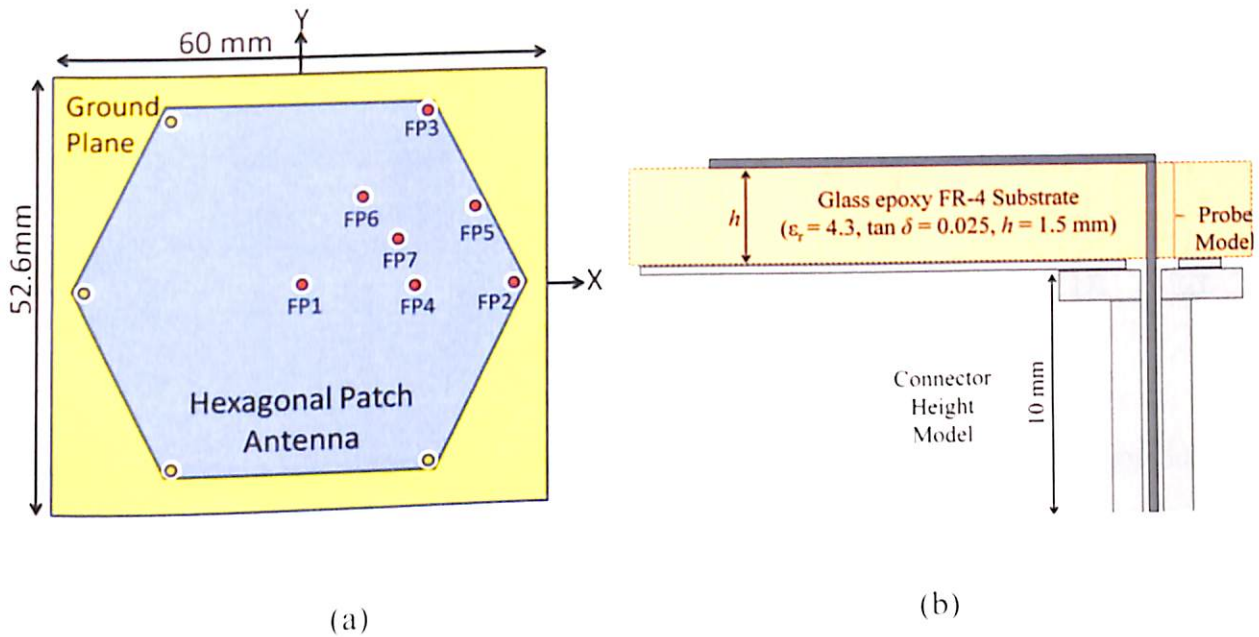


**Figure 2.2.** (a) Geometry of the proposed hexagonal-shaped patch antenna with the feed points indicated (b) Side view.

The pentagonal and hexagonal patch antenna are simulated with a rectangular ground plane on CST MWS simulation software to study the effect of probe feeding on various parameter like reflection coefficient, impedance and gain. The results show that the reflection coefficient is below -10 dB for a wideband of 8.6 GHz ranging from 11.4 to 20 GHz when polygons are fed at the vertices i.e. FP2 and FP3 as indicated in Figure 2.3 and Figure 2.4.

Both polygonal designs are simulated by changing the coordinates of feed point, from 0 to 26.5 mm on the radial distance from origin to vertex. It is observed that, the wideband antenna performance is obtained at 26 mm i.e. close to vertex. Feed point is also moved along the edge as well as from origin to midpoint of the edge. But multiband operation instead of broadband operation is observed at feed points other than at vertex of polygon.



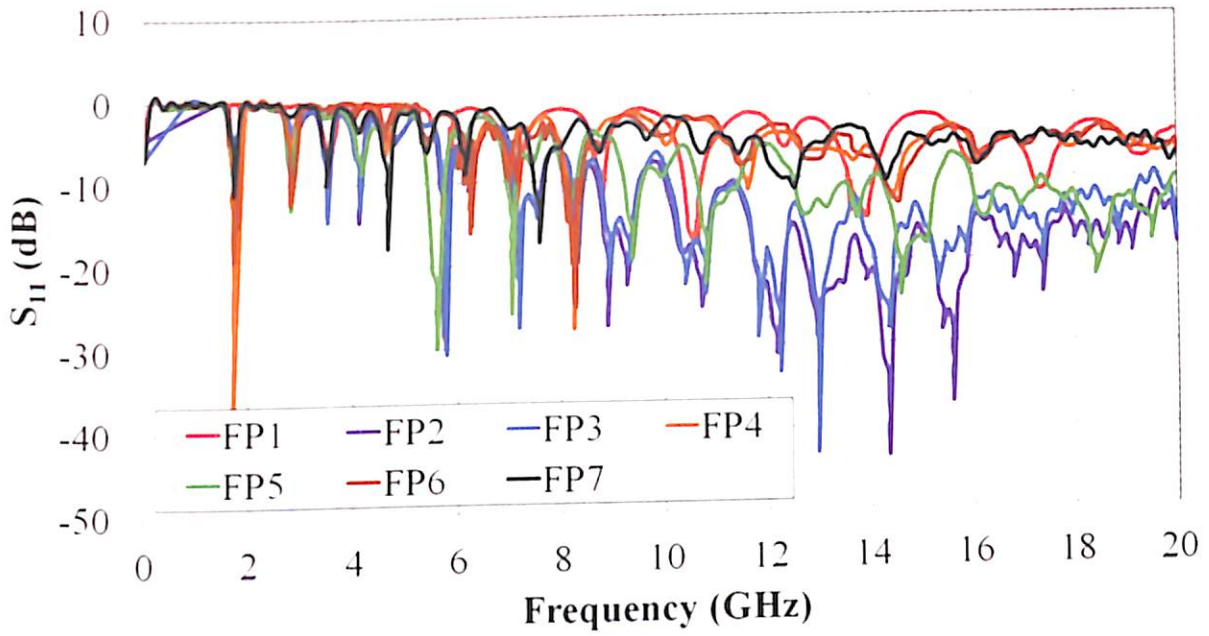


Figure 2.3. Simulated reflection coefficient with different probe feeding positions for pentagonal-shaped patch.

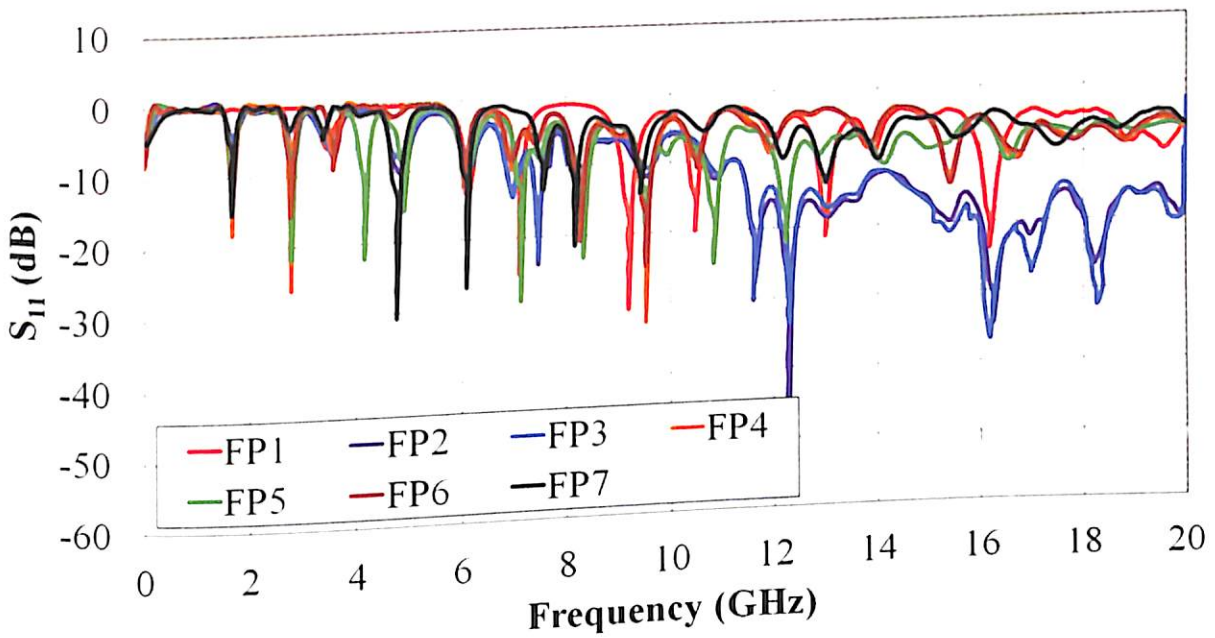
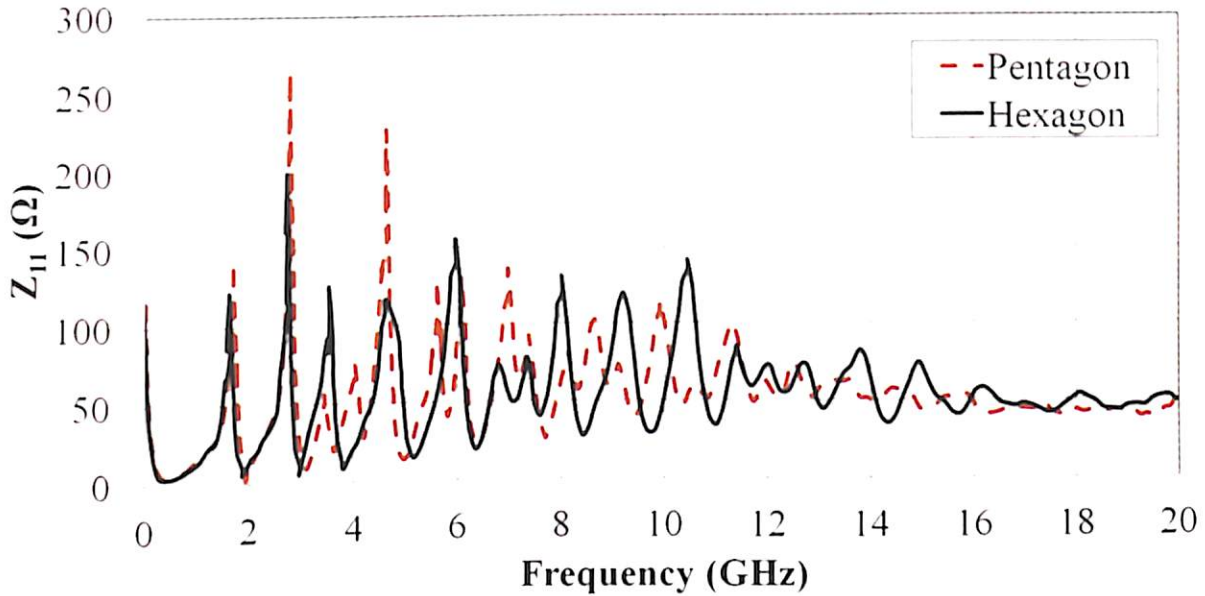
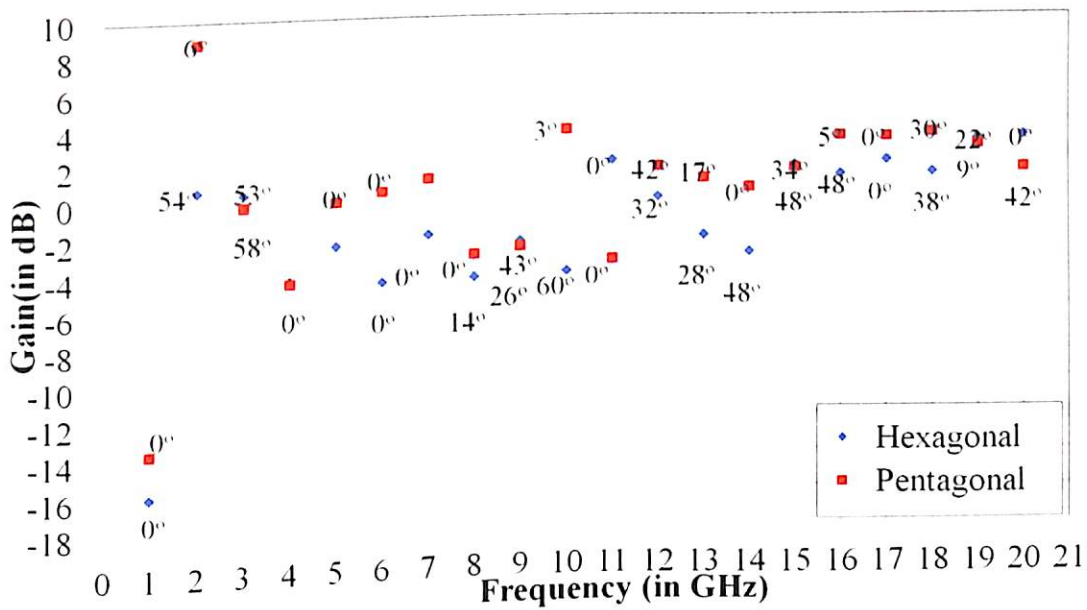


Figure 2.4. Simulated reflection coefficient with different probe feeding positions for hexagonal-shaped patch.

One of the significant parameters for patch antenna design is matching impedance to transmission line. The simulation result shows that impedance oscillates closely around 50  $\Omega$  in band of 11.4 to 20 GHz for both polygonal patches as indicated in Figure 2.5.



**Figure 2.5.** Simulated impedance for pentagonal and hexagonal patches at FP2/FP3.



**Figure 2.6.** Simulated Gain (in dB) for hexagonal and pentagonal patch at FP2/FP3.

To demonstrate the effect of the probe feeding on gain (in dB), both polygonal patch designs are simulated and the values discovered are displayed along with the main lobe



direction (in degrees) at which peak gain of antenna is observed in Figure 2.6. Positive gain for both patch geometries is noticed at band where impedance is perfectly matched.

### 2.3. Performance Comparison of Antennas for L-Band Applications

A circular patch is designed with radius of 100.2 mm to operate at 1.5 GHz, i.e. center frequency of L-Band as a uniform point of reference. Other polygonal patches are designed as if the circular radiator is perturbed at circumference but circumradius of each patch ( $V_r$ ) is further optimized to achieve centre frequency of the L-Band. The edge dimensions of ground plane ( $G_d$ ) and substrate ( $S_d$ ) exceeds are twice of  $V_r$  by 10 mm and 20 mm respectively. The effect of increasing number of edges ( $N$ ) from  $N = 3$  to 6 within a limit of  $V_r = 100.2$  mm is studied. Basic polygonal antennas are designed in CAD environment provided by CST MWS software using a glass epoxy FR-4 substrate ( $\epsilon_r = 4.3$ ,  $\tan \delta = 0.025$ ) of thickness 1.55 mm with conductor thickness of 0.015 mm on both sides of epoxy. The radius of the center pin of SMA connector is 0.65 mm, the radius while of dielectric ring used in SMA connector is 2.175 mm. The radius of outer conductor is 3.175 mm while the total height of SMA connector is 13.5 mm. The dimensions of the polygonal patch antennas are presented in Table 2.1. The polygonal designs are optimized by varying feed angle ( $F_q$ ) from 0 to  $2*\pi/2*N$  with the step of  $2*\pi/8*N$  for one sector of the polygon.

The feed angle ( $F_q$ ) is the angle between  $F_r$  and  $x$ -axis in anticlockwise direction as shown in Figure 2.7. The feed point ( $F_r$ ) is the distance from the origin to the location of feed. Finally, total thickness of antenna designed is 0.0079 times the free space wavelength of the center operating frequency 1.5 GHz.

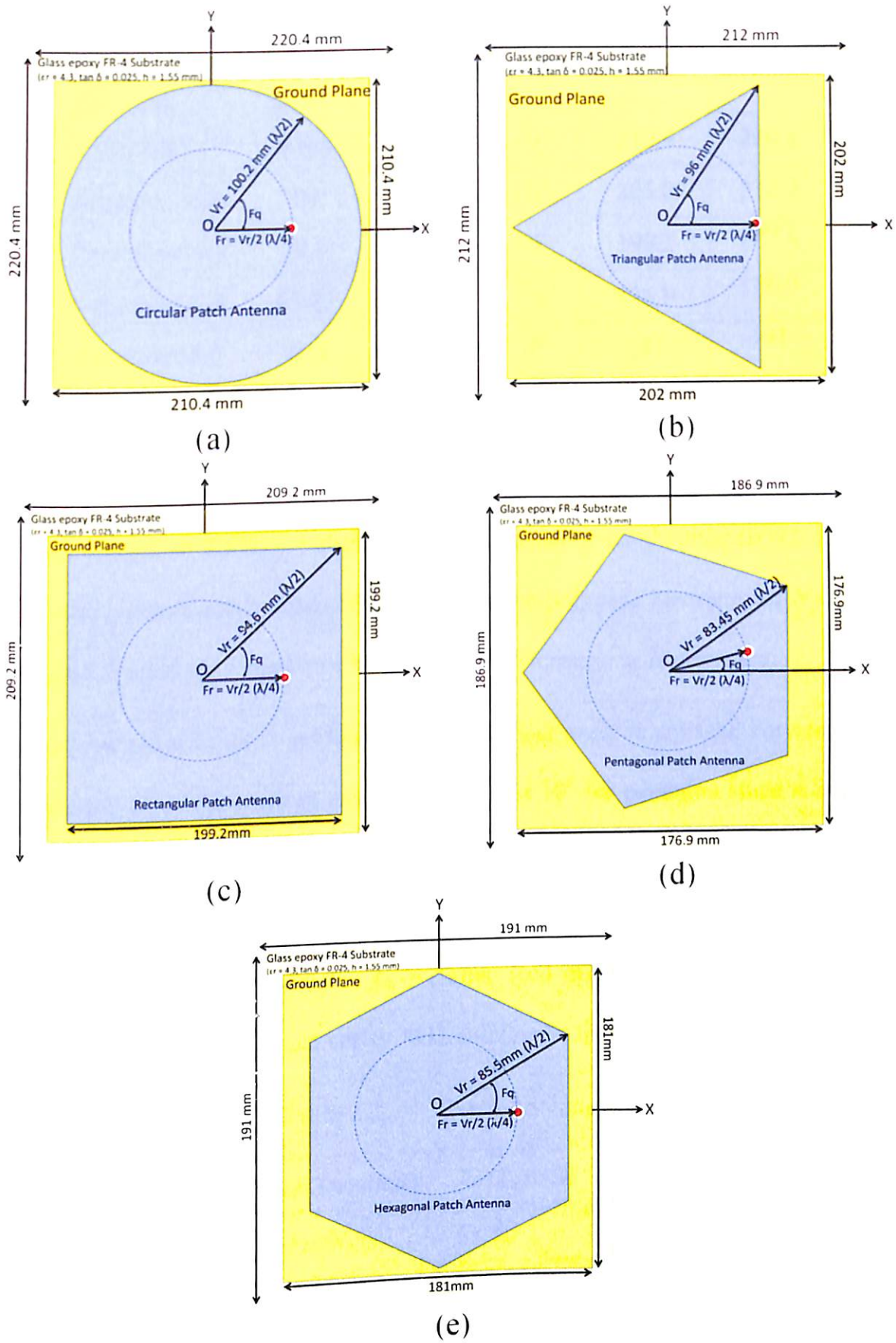


Figure 2.7. Schematic of (a) Antenna:  $A_1$  (b) Antenna:  $A_2$  (c) Antenna:  $A_3$  (d) Antenna:  $A_4$  (e) Antenna:  $A_5$ .

Table 2.1. Patch Antenna Design

$N$	Patch Geometry	$V_r$ (mm)	$F_r$ (mm)	$(V_r/2)$	$F_q$ (°)	$G_d$ (mm)	$S_d$ (mm)	BW (%)
$\infty$	Circle ( $A_1$ )	100.2	50.1	0	0	210.4	220.4	0.66
3	Triangle ( $A_2$ )	96	48	0	0	202.0	212.0	0.79
4	Rectangle ( $A_3$ )	94.6	47.3	0	0	199.2	209.2	0.79
5	Pentagon ( $A_4$ )	83.45	41.725	18	18	176.9	186.9	0.84
6	Hexagon ( $A_5$ )	85.5	42.75	0	0	181	191	2.28

The optimum values of  $F_q$  for the antenna  $A_1$ ,  $A_2$ ,  $A_3$ ,  $A_4$  and  $A_5$  at center frequency of 1.5 GHz are indicated in Table 2.1 along with the impedance bandwidths (BW). It is observed that if a feed point is selected near the edge then the polygons having even  $N$  display better performance in terms of impedance bandwidth that increases as  $N$  increases.

The polygons with odd  $N$  perform well when feed point is selected between vertex and center of edge.  $F_q$  is optimum at a different value at  $18^\circ$  for pentagon since it is asymmetric over the width of the ground plane but dimensions of pentagonal patch geometry favors compactness of antenna. Real part and the imaginary part of input impedance at a center frequency of 1.5 GHz for antennas  $A_1$ - $A_5$  after feed optimization are listed in Table 2.2. Hexagon has a real impedance closer to  $50 \Omega$  and lowest imaginary impedance.

Table 2.2. Patch Antennas Impedance

$N$	Patch Geometry	$Re(Z_{11})(\Omega)$	$Im(Z_{11})(\Omega)$
$\infty$	Circle ( $A_1$ )	51.56	-20.033
3	Triangle ( $A_2$ )	47.203	+16.299
4	Rectangle ( $A_3$ )	44.54	+16.65
5	Pentagon ( $A_4$ )	46.26	+9.285
6	Hexagon ( $A_5$ )	48.07	1.039

Similar to a rectangular patch antenna, any polygonal shaped patch antenna may be modeled as RLC equivalent circuit as shown in Figure 2.8. After applying equations given in (Garg 2001), values for lumped elements ( $R$ ,  $L$ , and  $C$ ) can be obtained for different polygonal patch antenna, as given by equations (2.1-2.3).

$$C = \frac{\epsilon_0 \epsilon_c A_c}{2h} \quad (2.1)$$

$$L = \frac{l}{(2\pi f_r)^2 C} \quad (2.2)$$

$$R = \frac{Q}{(2\pi f_r) C} \quad (2.3)$$

where,  $A_c$  is the effective overlapping area with ground of the polygonal patch,  $f_r$  is centre frequency of operating band, while height ( $h$ ) and dielectric constant ( $\epsilon_c$ ) are substrate characteristics, respectively.

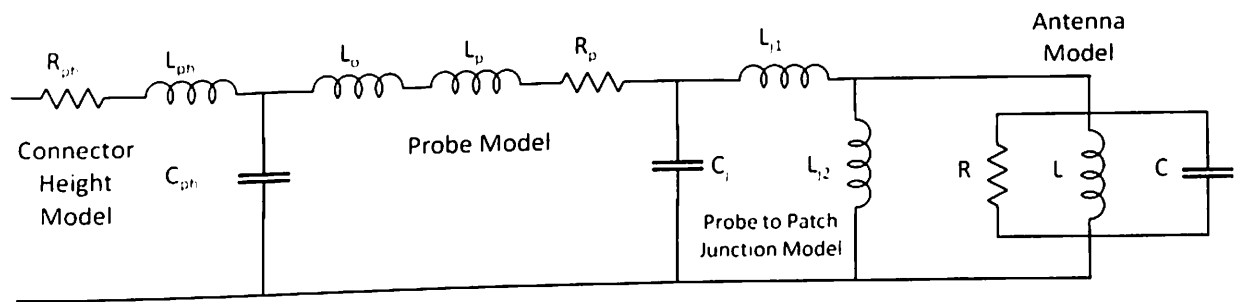


**Figure 2.8.** Equivalent Circuit model of the antennas at  $f = 1.5$  GHz for (a)  $A_1$  (b)  $A_2$  (c)  $A_3$  (d)  $A_4$  (e)  $A_5$ .

The probe can be modeled in three sections i.e. probe height model (Pozar 2014), probe model (Garg 2001) and probe to patch junction model (Pozar 2014). The probe height model is modeled as coaxial transmission line model by series resistance ( $R_{ph} = 0.03184 \Omega$ ), series inductance ( $L_{ph} = 2.42$  nH) and shunt capacitance ( $C_{ph} = 0.9663$  pF). The probe model is modeled as by series inductance ( $L_o = 3.42$  pH and  $L_p = 1.0161$  nH), resistance ( $R_p = 4.5894$

$\Omega$ ) as shown in Figure 2.8. The series inductors ( $L_s$  and  $L_p$ ) used to model the feed probe are proportional to the height of the dielectric substrate. The transition or junction between probe and the polygonal patch is modeled as shunt capacitance ( $C_j = 12.20$  pF), series inductance ( $L_{s1} = 0.298$  nH) and shunt inductance ( $L_{s2} = 0.641$  nH). The impedance of a probe height model and probe junction model can be calculated using the equations given in (Pozar 2014), while the impedance of the probe model can be evaluated using equations given in (Garg 2001).

Table 2.3. Patch Antennas  $RLC$  Values Shown in Figure 2.8

$N$	<b>Patch Geometry</b>	$R$ ( $\Omega$ )	$L$ (in pH)	$C$ (in nF)
$\infty$	Circle	38.53	29.06	0.38
3	Triangle	17.54	76.56	0.15
4	Rectangle	18.21	51.21	0.22
5	Pentagon	21	55.36	0.20
6	Hexagon	26	48.26	0.23

For antennas shown in Figure 2.7, equivalent values for  $R$ ,  $L$ , and  $C$  are indicated in Table 2.3. The input impedance ( $Z_{11}$ ) of antennas is evaluated using equivalent circuit model (ECM) considering  $RLC$  resonator resonating at 1.5 GHz. Impedance  $Z_{11}$  is plotted in Smith Chart (SC) for all antennas as shown in Figure 2.9. It is observed that at resonating frequency, the circle and all polygonal patch geometries are intersecting the unit circle which suggests that impedance value is close to  $50 \Omega$  but is reactive, while curve for hexagon is intersecting the zero imaginary line which suggests lowest reactive impedance value as shown in Figure 2.9 and as suggested by Table 2.2.

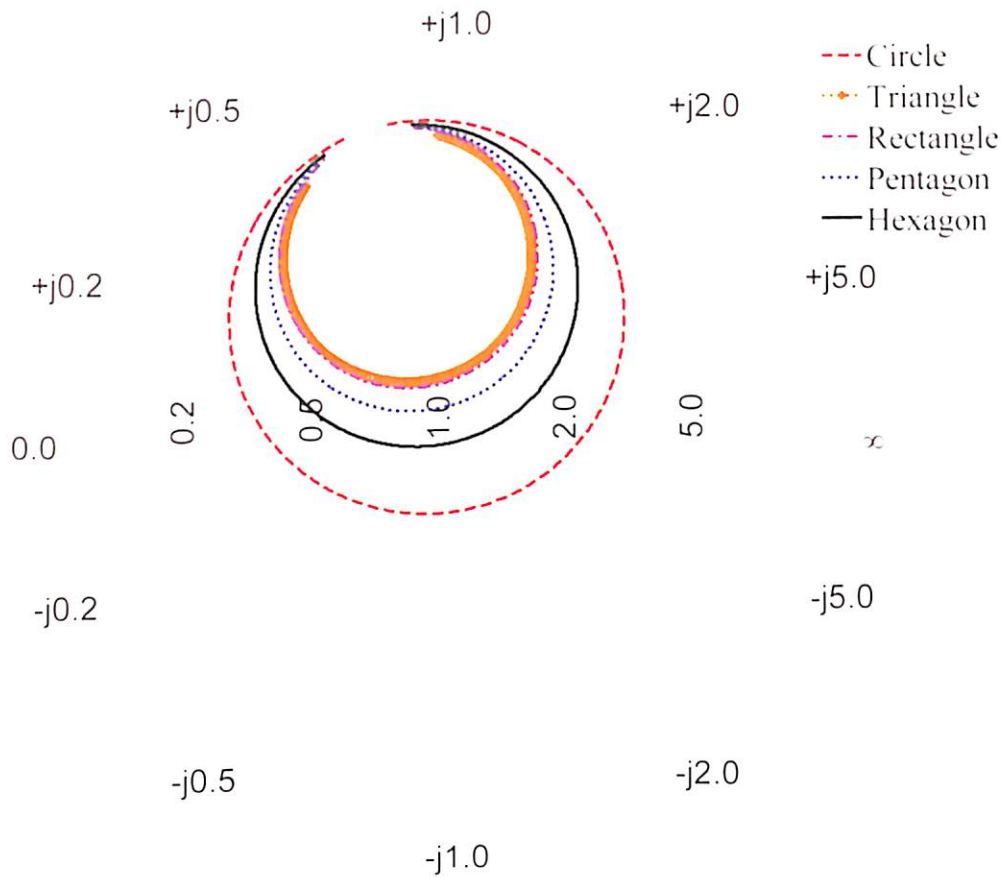


**Figure 2.9.** SC of A1 compared with the results of A2, A3, A4 and A5 using Equivalent circuit model.

Further, the effect of polygonal geometries on of reflection coefficient ( $S_{11}$ ), impedance ( $Z_{11}$ ), farfield gain and directivity is studied and the results are compared and analyzed through simulations on CST MWS.

Figure 2.10 shows the reflection coefficient ( $S_{11}$  in dB) of all antennas  $A_1$ ,  $A_2$ ,  $A_3$ ,  $A_4$  and  $A_5$ . It is observed from the plot that scattering characteristics of polygonal patch antennas are dependent on shape of patch, moreover, on number of edges,  $N$ . The hexagonal shaped patch antenna has the largest bandwidth among  $A_1$  to  $A_5$ . High bandwidth of the hexagon is due to dual but proximate resonances, one at 1.50 GHz and other at 1.52 GHz. Reflection coefficient (in dB) value decreases as the value of  $N$  is increased from 3 to 6 as shown in Figure 2.10. Hexagonal and pentagonal shaped patch antenna exhibit low value of reflection coefficient as



compared to circle, while triangular and rectangular patches have reflection coefficients of same order as that of circular radiator.

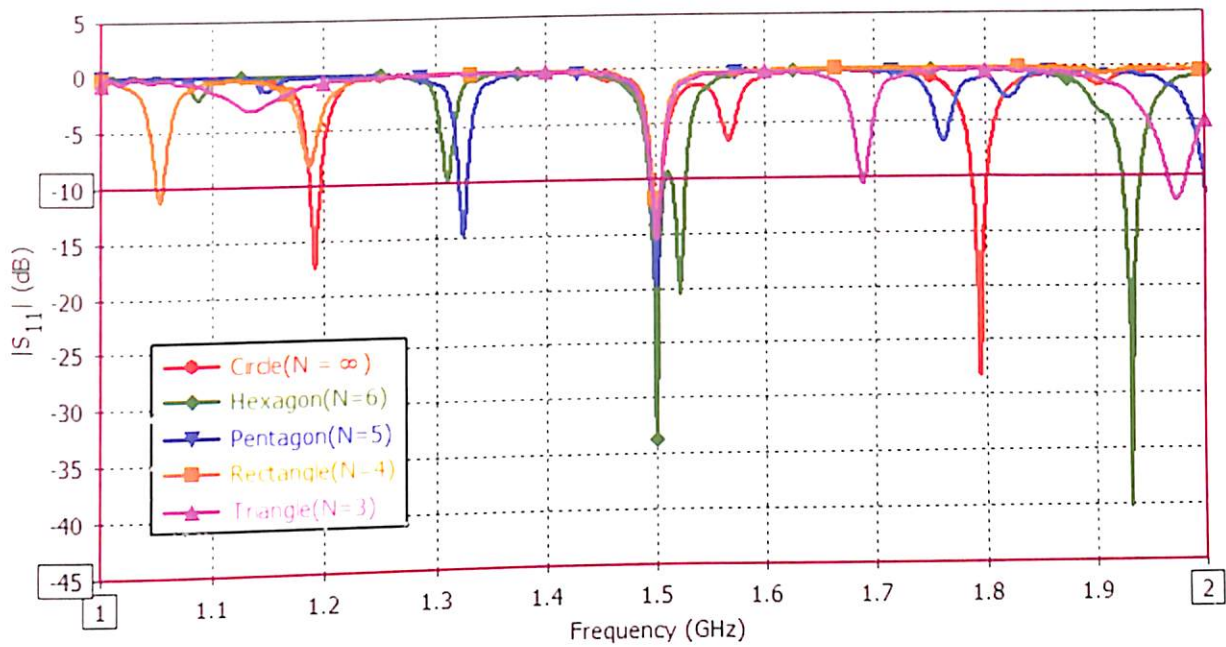


**Figure 2.10.** The  $S_{11}$  (in dB) of  $A_1$  compared with the  $S_{11}$  of  $A_2$ ,  $A_3$ ,  $A_4$  and  $A_5$ .

Impedance matching is one of the prime objectives of an antenna design when fed through a direct RF probe. The impedances ( $Z_{11}$  in  $\Omega$ ) are evaluated for all proposed designs,  $A_1$ ,  $A_2$ ,  $A_3$ ,  $A_4$  and  $A_5$  as discussed in earlier and are compared in Figure 2.11. It is observed that value of  $Z_{11}$  (real and imaginary part) at 1.5 GHz, is  $48.07 + 1.039j \Omega$  for  $A_5$  which suggest hexagon more suitable than the other antenna geometries.

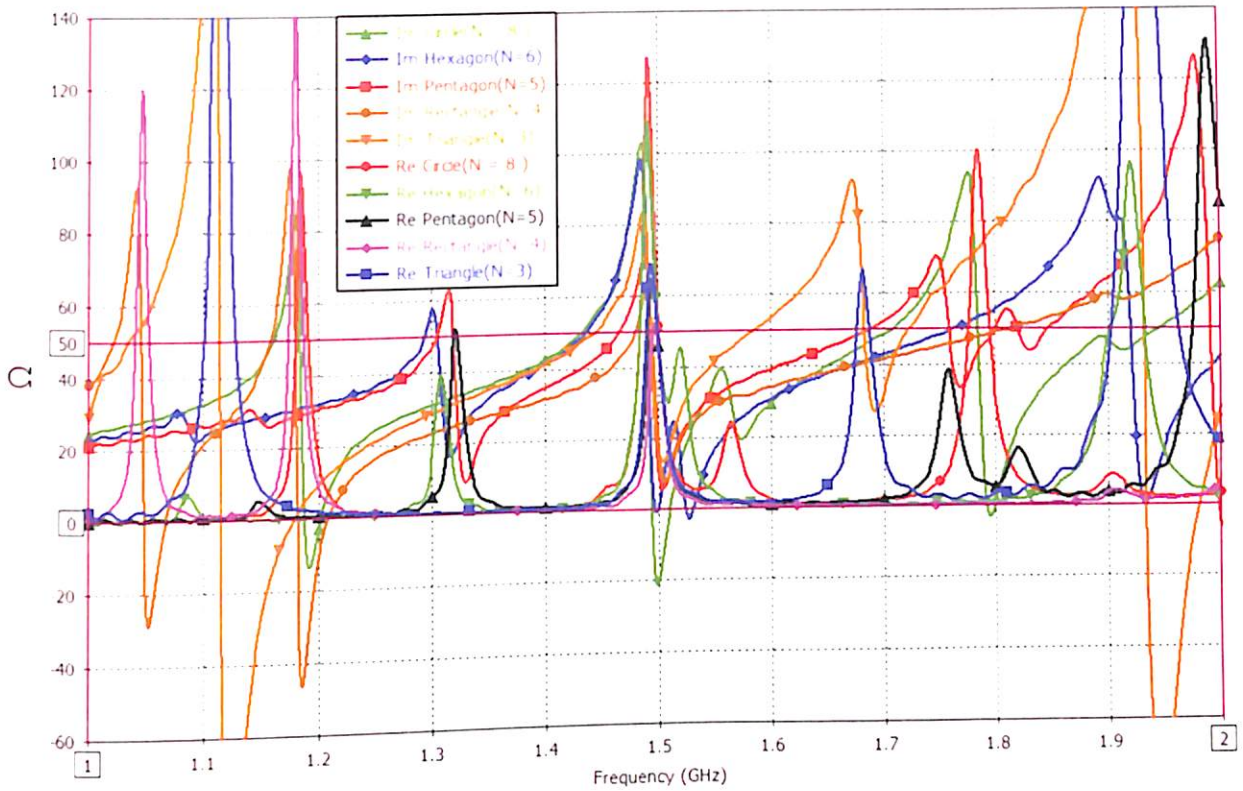


**Figure 2.11.** The  $Z_{11}$  of A1 compared with the  $Z_{11}$  of A2, A3, A4 and A5.

The impedance is highly capacitive for antenna A<sub>1</sub>, inductive for A<sub>2</sub>, highly inductive for A<sub>3</sub> and inductive for A<sub>4</sub> at 1.5 GHz as observed in SC shown in Figure 2.12. Probe can be modeled by series inductance due to which, all the loops lie in the inductive region of SC as shown in Figure 2.12. Comparing, SC (Figure 2.9) derived from equivalent circuit model, with SC (Figure 2.12) generated using simulation results, it is observed that probe inductance dominates and requires compensation. Two loops are observed in simulation results of circular and hexagonal patch antenna, those are indicating adjacent resonances near 1.5 GHz.

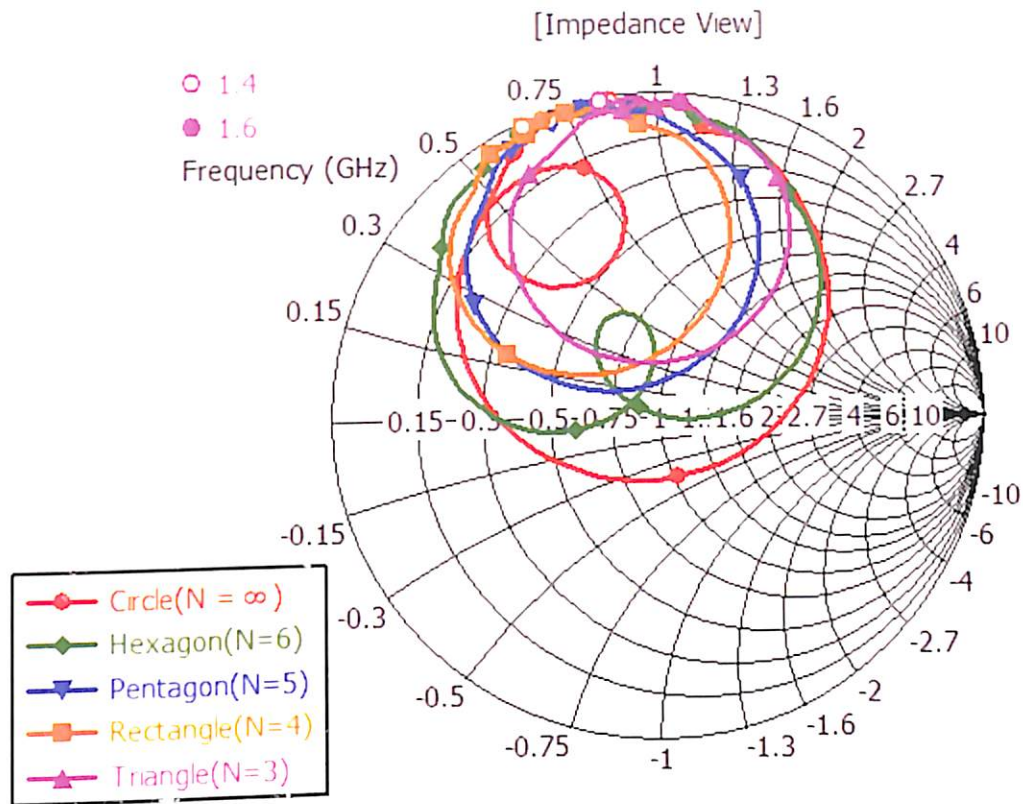


**Figure 2.12.** The SC of A1 compared with the SC of A2, A3, A4 and A5.

The effect of patch geometry on farfield gain (in dB) is shown in Figure 2.13, where the gain points displayed in figure are observed at distant main lobe direction in radiation pattern evaluated at a common frequency of 1.5 GHz for different values of  $N$ . It is interesting to observe that although triangular and hexagonal patches have lower ratio of patch to ground plane area, they provide higher gain compared to other patch geometries as shown in Table 2.4. Hexagonal shaped patch has positive gain of 0.16 dB while the triangular patch antenna has a gain of 1.7 dB at 1.5 GHz.



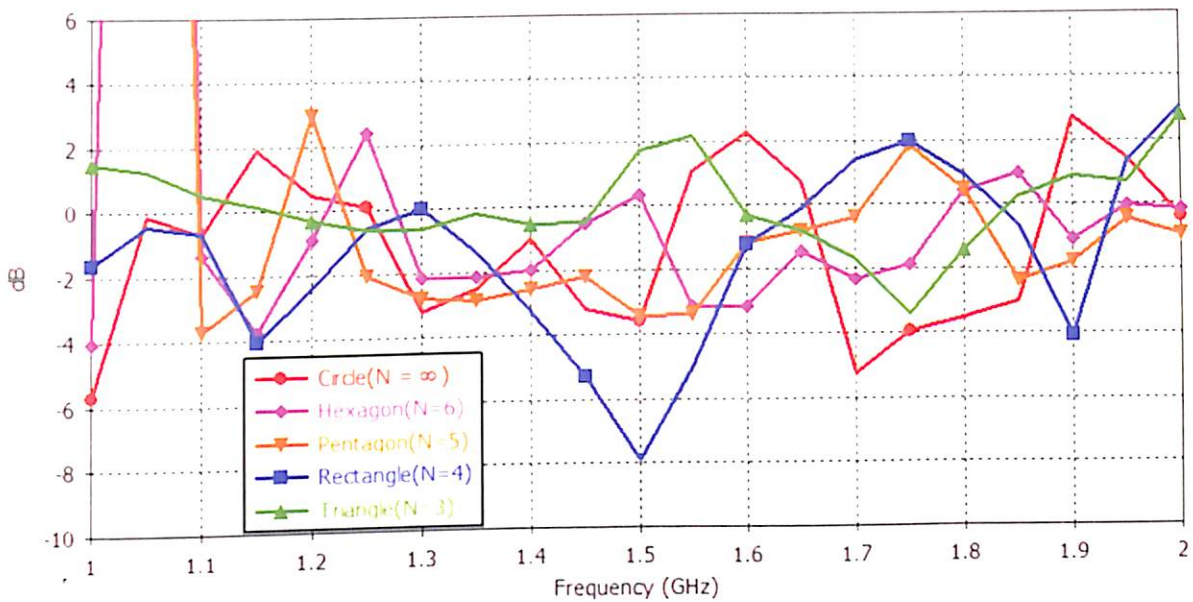


**Figure 2.13.** The farfield gain of A1 compared with the gain of A2, A3, A4 and A5.

The farfield directivity of patch antennas is shown in Figure 2.14. The triangular patch antenna (8.9 dBi) and hexagonal patch antenna (7.58 dBi), both are more directive compared to others. Directivity decreases with increase in the ratio of patch to ground plane area with an exception of rectangular radiator. Pentagonal (5.16 dBi) and rectangular (1.48 dBi) patch are less directive as compared to circular radiator (6.06 dBi). The 3-dB beam-width of circular patch is  $34.3^\circ$  in main lobe direction of  $30^\circ$  at frequency of 1.5 GHz with three side lobes with level less than -6.7 dB. In case of hexagonal patch, the 3-dB beam-width is  $54.6^\circ$  in main lobe direction of  $0^\circ$  at frequency of 1.5 GHz with side lobes with level less than -8.9 dB. The circular and rectangular have null at  $0^\circ$  as shown in Figure 2.14. It is observed that the performance of triangular and hexagonal patch antennas are comparable but the beam-width of hexagonal patch is less than that of triangular radiator. Table 2.4 summarizes comparison of all patch antennas discussed in section 2.3 on basis of gain (in dB), directivity (in dBi), efficiency and beam-width (in degrees) at 1.5 GHz.

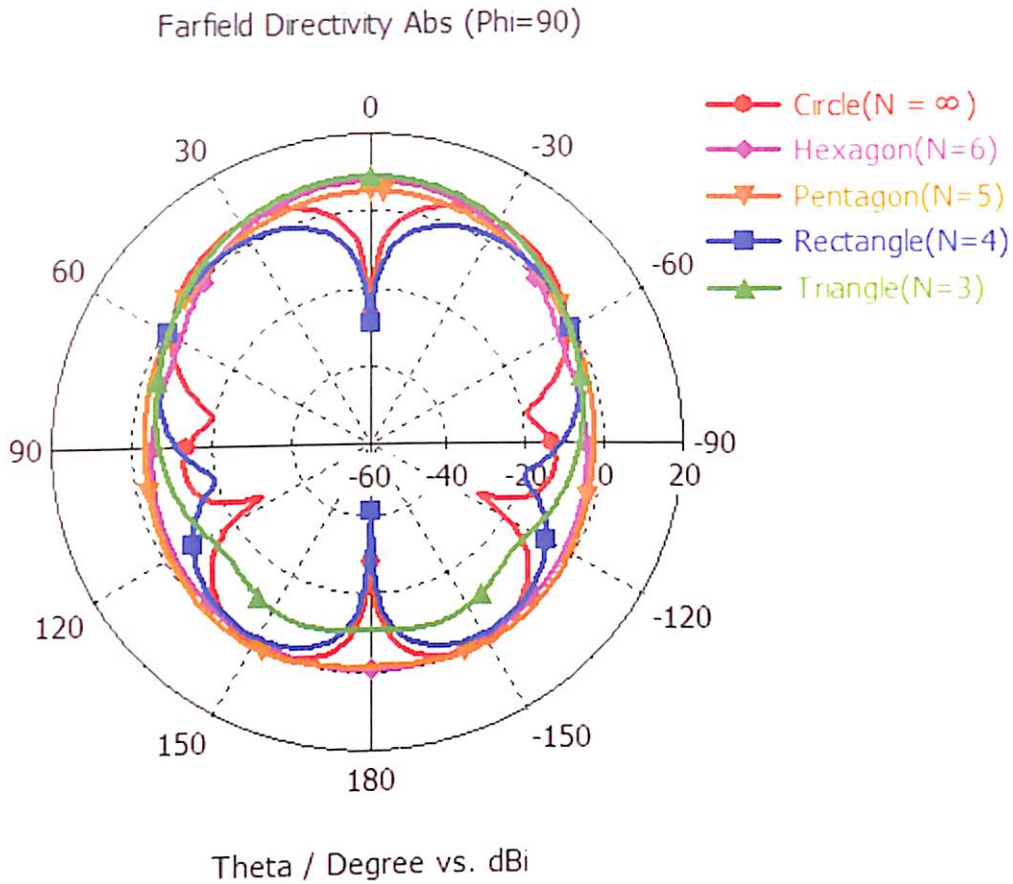


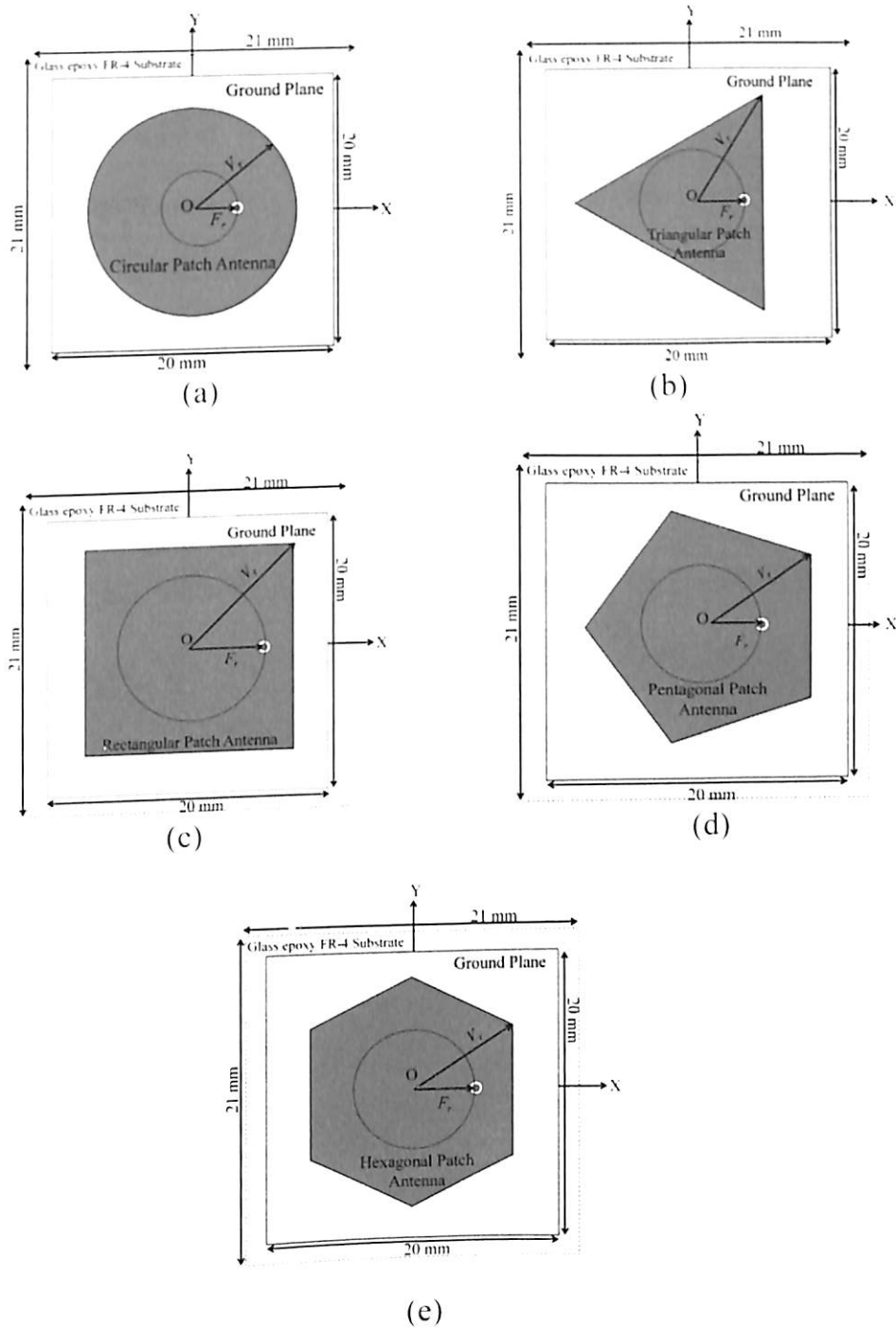
Figure 2.14. The farfield directivity of  $A_1$  compared with the results of  $A_2, A_3, A_4, A_5$ .

Table 2.4. Performance comparison of L-band patch antennas

$N$	Patch Geometry	Ratio of Patch to Ground Area	Gain (in dB)	Directivity (in dBi)	Efficiency ( $\eta$ )	Beam-width ( $\theta$ )( $^\circ$ )
$\infty$	Circle	0.7115	-4.32	6.06	0.0814	34.3
3	Triangle	0.2940	1.71	8.88	0.1779	58.6
4	Rectangle	0.4511	-9.96	1.48	0.0706	45.2
5	Pentagon	0.5304	-3.54	5.16	0.1215	69.6
6	Hexagon	0.5799	0.0744	7.58	0.1683	54.6

## 2.4. Performance Comparison of Antennas for X-Band Applications

To analyze antennas discussed in section 2.3 when fundamental mode is radiated, the dimensions of antennas are chosen such that they radiate in X-Band at 8.5 GHz antenna where dimensions are presented in Table 2.5.



**Figure 2.15.** Schematic of (a) Antenna:  $A_1$  (b) Antenna:  $A_2$  (c) Antenna:  $A_3$  (d) Antenna:

$A_4$  (e) Antenna:  $A_5$ .



Table 2.5. X-band Patch Antennas Design

$N$	Patch Geometry	$V_r$ (mm)	$F_r$ (mm)	$L_g$ (mm)	$L_s$ (mm)
$\infty$	Circle ( $A_1$ )	4.35	1.7	20	21
3	Triangle ( $A_2$ )	5.70	1.7	20	21
4	Rectangle ( $A_3$ )	5.28	1.6	20	21
5	Pentagon ( $A_4$ )	4.90	1.6	20	21
6	Hexagon ( $A_5$ )	4.73	1.6	20	21

The results obtained after simulation on CST MWS are compared to study the effect of all patch geometries on reflection coefficient ( $S_{11}$ ), impedance ( $Z_{11}$ ), farfield gain.

Scattering characteristics of antennas are dependent on shape of patch. The effect over reflection coefficient,  $S_{11}$  with change in  $N$  can be observed in Figure 2.16. The hexagonal shaped patch antenna has the largest Bandwidth among  $A_1$  to  $A_5$ . Hexagonal shaped patch antenna exhibit low value of reflection coefficient as compared to circle, while triangular and rectangular patches have high reflection as compared to circular radiator.

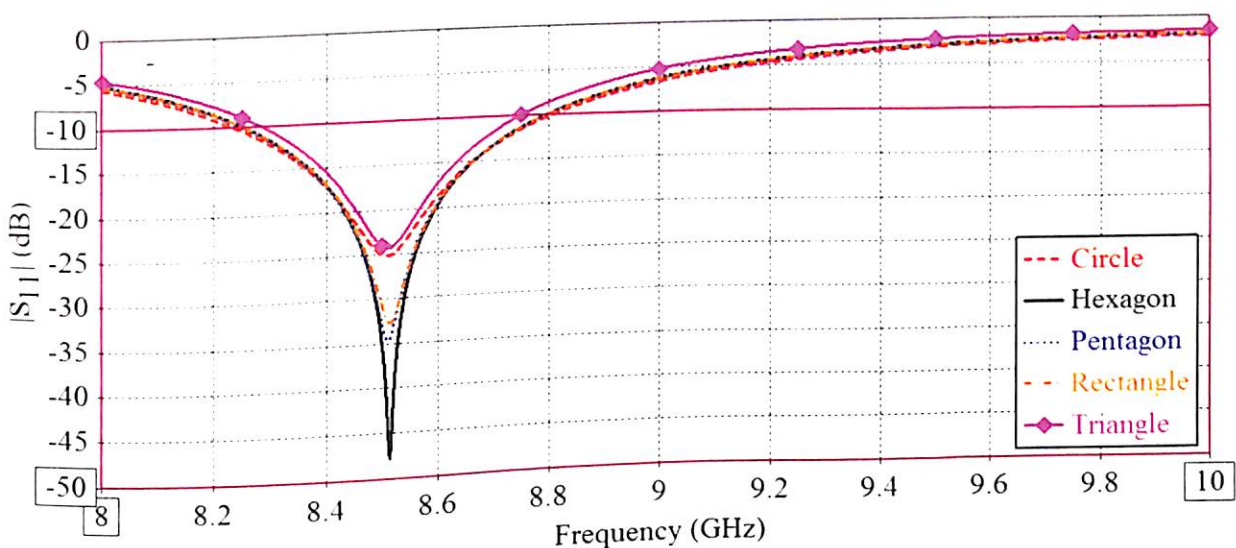
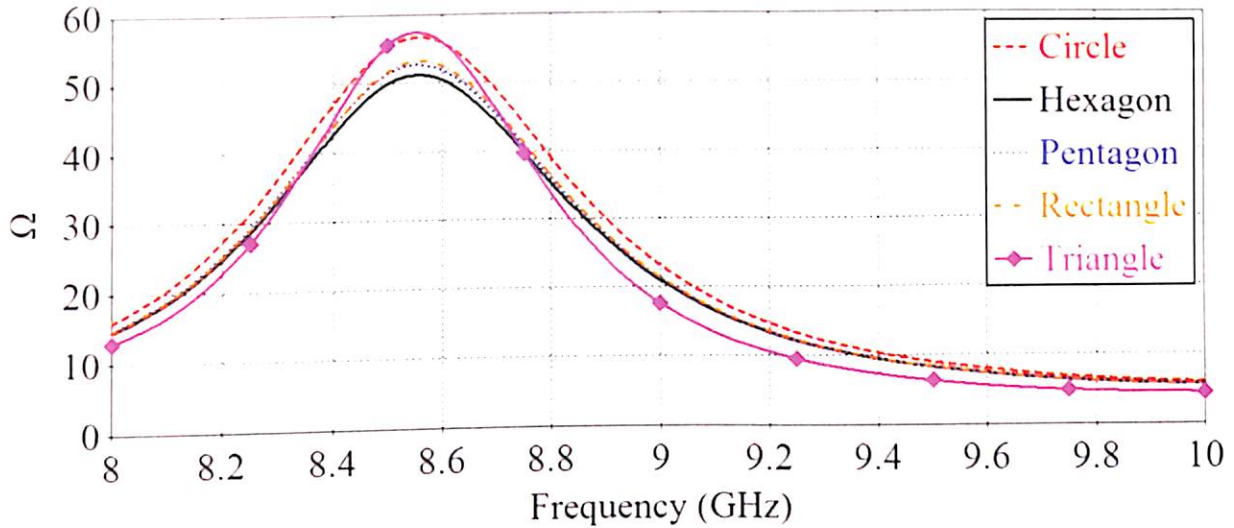
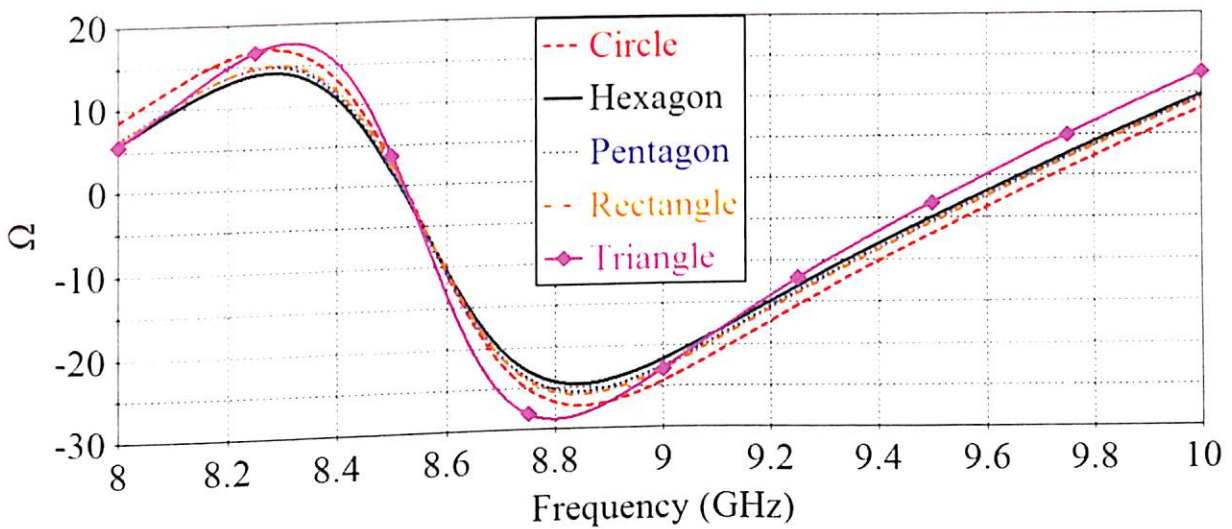


Figure 2.16. The  $S_{11}$  (in dB) of  $A_1$  compared with the  $S_{11}$  of  $A_2$ ,  $A_3$ ,  $A_4$  and  $A_5$ .

The impedances are evaluated for all proposed designs and are compared in Figure 2.17. Design  $A_1$ ,  $A_2$ ,  $A_3$  and  $A_4$  shows resistive impedance at resonating frequency as observed in SC shown in Figure 2.18. All the loops are touching unit circle of the SC as reflected in Figure 2.18.



(a)



(b)

**Figure 2.17.** The  $Z_{11}$  of  $A_1$  compared with the  $Z_{11}$  of  $A_2$ ,  $A_3$ ,  $A_4$  and  $A_5$  (a) Real Part (b) Imaginary part.

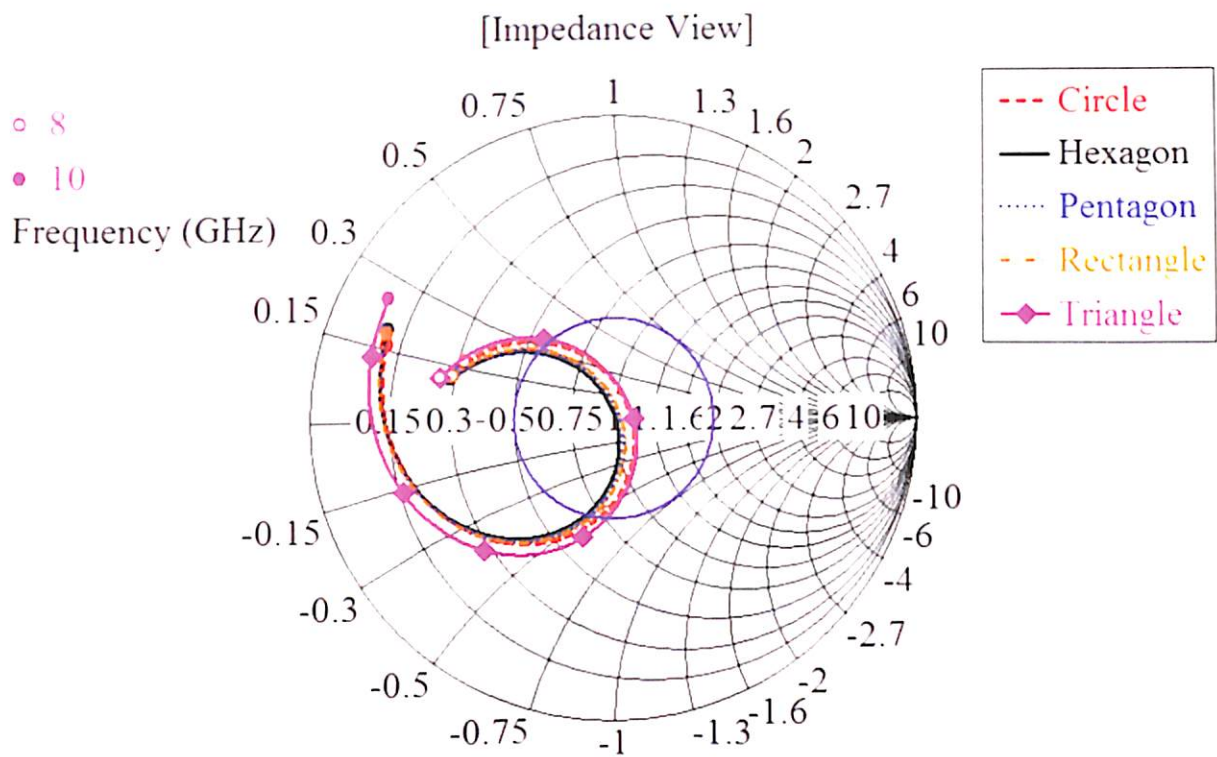


**Figure 2.18.** The SC of  $A_1$  compared with the SC of  $A_2$ ,  $A_3$ ,  $A_4$  and  $A_5$ .

The effect of patch geometry on farfield gain (in dB) is shown in Figure 2.19, where the gain points displayed for all antennas are observed at main lobe direction in radiation pattern evaluated at a common frequency of 8.5 GHz. The gain is comparable for all antennas except triangle which exhibit lower gain.

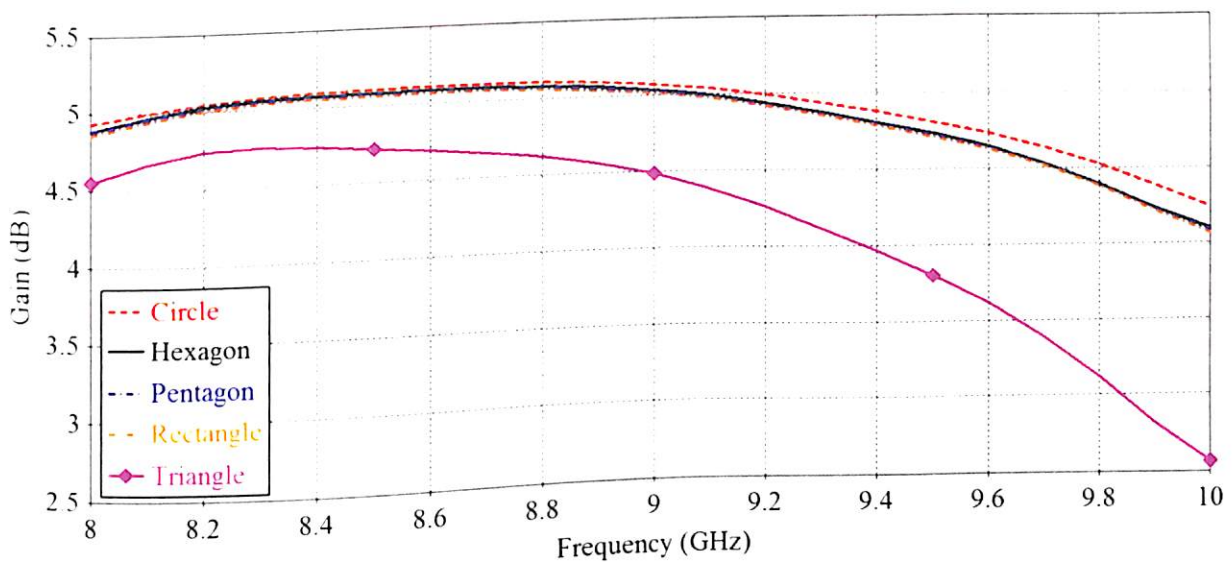
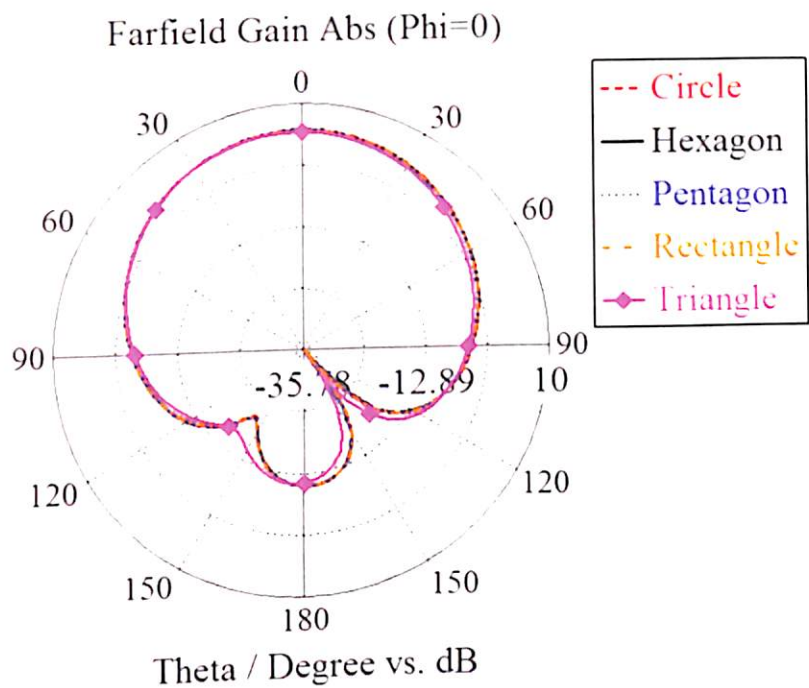
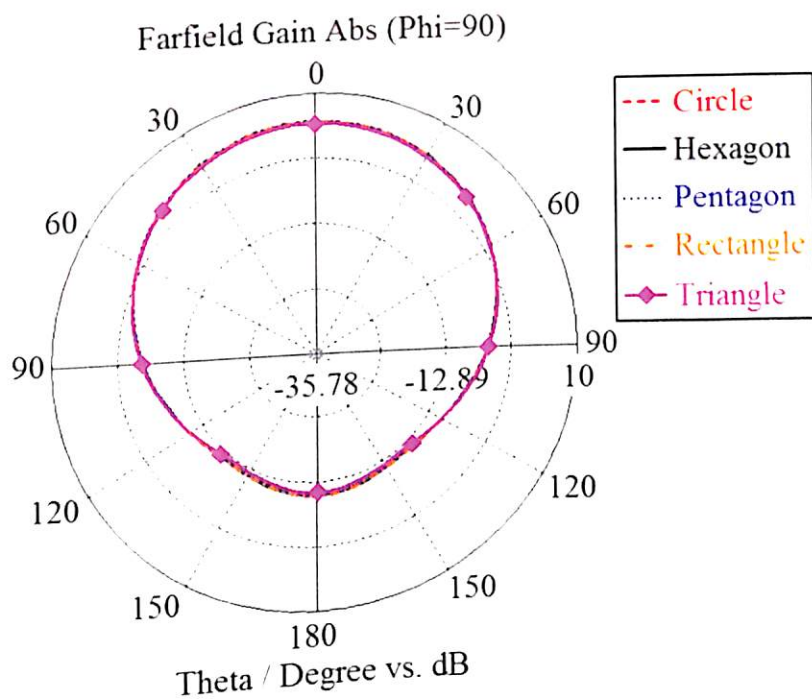


**Figure 2.19.** The farfield gain of  $A_1$  compared with the gain of  $A_2$ ,  $A_3$ ,  $A_4$  and  $A_5$ .

The radiation pattern of proposed patch antennas at two fundamental plane i.e. E and H-plane are shown in Figure 2.20. All design have similar radiation pattern due to fundamental mode radiation as shown in Figure 2.20.



(a)



(b)

**Figure 2.20.** The farfield radiation pattern of  $A_1$  compared with the results of  $A_2, A_3, A_4,$

$A_5.$



Table 2.6 summarizes performance comparison of all patch antennas discussed earlier on basis of gain (in dB), directivity (in dBi), efficiency and beam-width (in degrees) at the center frequency of X-Band.

Table 2.6. Performance comparison of X-band antennas

<i>N</i>	<i>Patch Geometry</i>	<i>Ratio of Patch to Ground Area</i>	<i>Gain (in dB)</i>	<i>Directivity (in dBi)</i>	<i>Efficiency (<math>\eta</math>)</i>	<i>Beam-width (<math>\theta</math>)(<math>^{\circ}</math>)</i>
2	Circle	0.152	5.1	6.55	0.7786	86.7
3	Triangle	0.109	4.75	6.5	0.7307	89.3
4	Rectangle	0.140	5.06	6.55	0.7725	86.7
5	Pentagon	0.145	5.07	6.54	0.7752	86.8
6	Hexagon	0.148	5.08	6.54	0.7767	86.7

## 2.5. Edge Perturbation Effect in Polygonal Patch Antennas

CST MWS software used to design pentagonal and hexagonal patches, is again used to simulate antenna designs based on both patch geometries and their transformations. The simulated results obtained are observed and analyzed to study the effect of change in geometry i.e., from polygon to polygram, on reflection coefficient ( $S_{11}$ ), impedance ( $Z_{11}$ ) and far field gain (in dB). Both polygonal patch antennas are simulated with a rectangular ground plane and substrate with same dimensions. The performance of the antenna is analyzed by feeding a vertex of polygon through a direct coaxial probe, in context to identify operating multiband or wideband characteristics of the designs in objective for analysis. It is observed during simulations that the presence of feed points indicated by yellow (light) color points do not have significant effect on the performance of the antenna in context to the broad band that is subject of interest.

In order to understand the performance characteristics of polygonal patch i.e. pentagon and hexagon, the edges are perturbed such the regularity in shape is maintained. The antenna in Figure 2.21 is assumed to use a glass epoxy FR-4 substrate ( $\epsilon_r = 4.3$ ,  $\tan \delta = 0.025$ ) of thickness 1.5 mm with an area of  $80 \times 80 \text{ mm}^2$ . The size of the ground plane is  $60 \times 52.6 \text{ mm}^2$ . All the feed points are kept closer to vertices of pentagon at a radial distance of 26 mm from the center of pentagon. The change in geometry of polygon was introduced by varying coordinates of midpoints ( $vm$ ) of edges of polygons so that the midpoint moves on a trajectory towards center of polygon ' $O$ ' radially. This results an interior vertex in between two exterior vertices of polygon. An angle,  $\theta$  is formed at each edge of polygon which lies between two exterior vertices and one interior vertex. All the interior vertices of pentagram (dashed line star geometry in Figure 2.21) are moved from ' $vm$ ' to ' $O$ ' in steps of difference of 1 mm on the radial (dotted) line as shown in Figure 2.21, to investigate the effect of change in antenna geometry on antenna's performance. The distance indicated by a dotted line between ' $vm$ ' and ' $O$ ' in Figure 2.21 is 21.8 mm for a pentagon with radial distance  $R = 27 \text{ mm}$ .

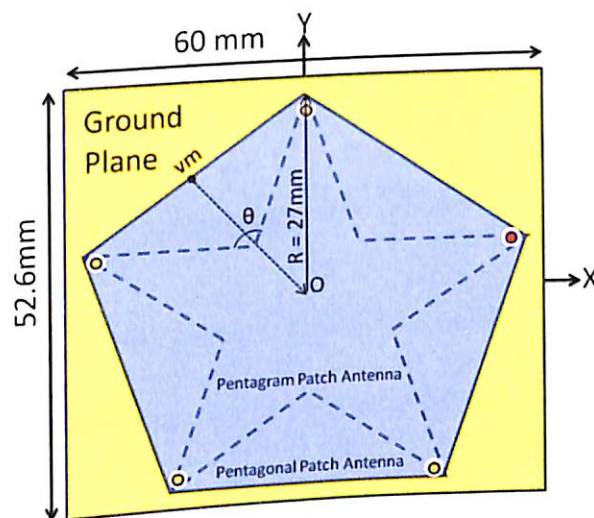


**Figure 2.21.** Pentagon to pentagram schematic.

Similar to the schematic of Figure 2.21, a polygonal patch with six edges and six vertices, i.e., hexagonal patch is designed with a radial distance of 27 mm from center to its vertex as



shown in Figure 2.22. The ground plane, substrate material and their dimensions are kept same as for pentagonal patch discussed earlier in pentagonal. The feed points are kept at a radial distance of 26 mm from center of hexagon close to its vertices. To analyze the effect of change in geometry on hexagonal patch antenna, the hexagram interior vertices are moved in steps of 1 mm distance from 23.38 mm, the distance of midpoint of edge 'vm' of hexagon from center of hexagon, towards the center of hexagon 'O' as shown in Figure 2.22. The midpoints of edges of polygon are defined using variable coordinates to maintain equal radial distance from center of polygon to all interior vertices every time any iteration for simulation is performed.

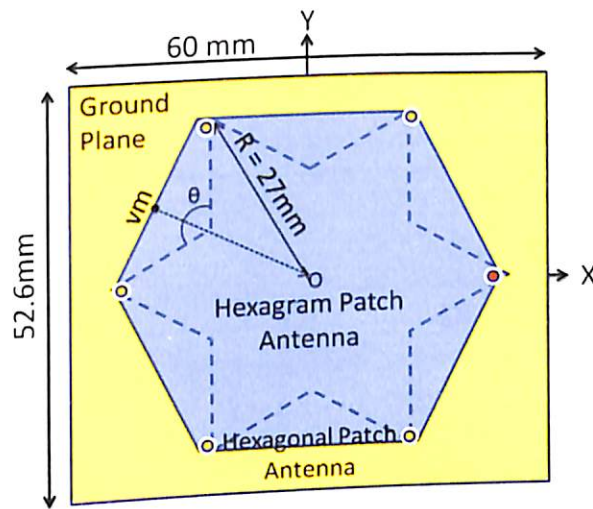


**Figure 2.22.** Hexagon to hexagram schematic.

Scattering characteristics of a polygonal antenna is sensitive to geometrical perturbations as may be seen in Figure 2.23 and Figure 2.24 for pentagonal and hexagonal patch antennas respectively.

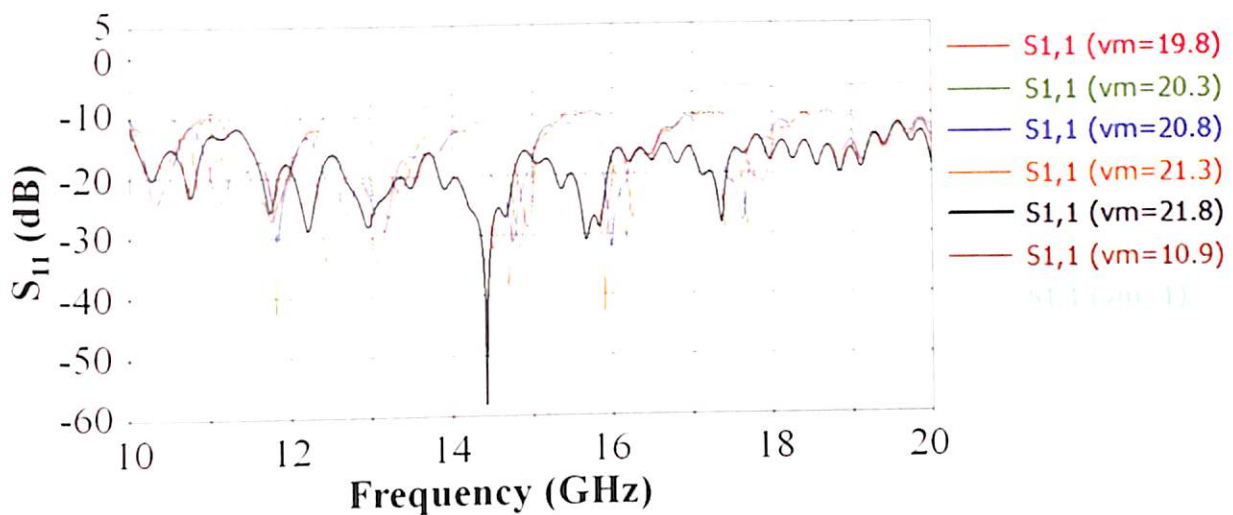


Figure 2.23. Simulated reflection coefficient (in dB) for pentagon to pentagram.

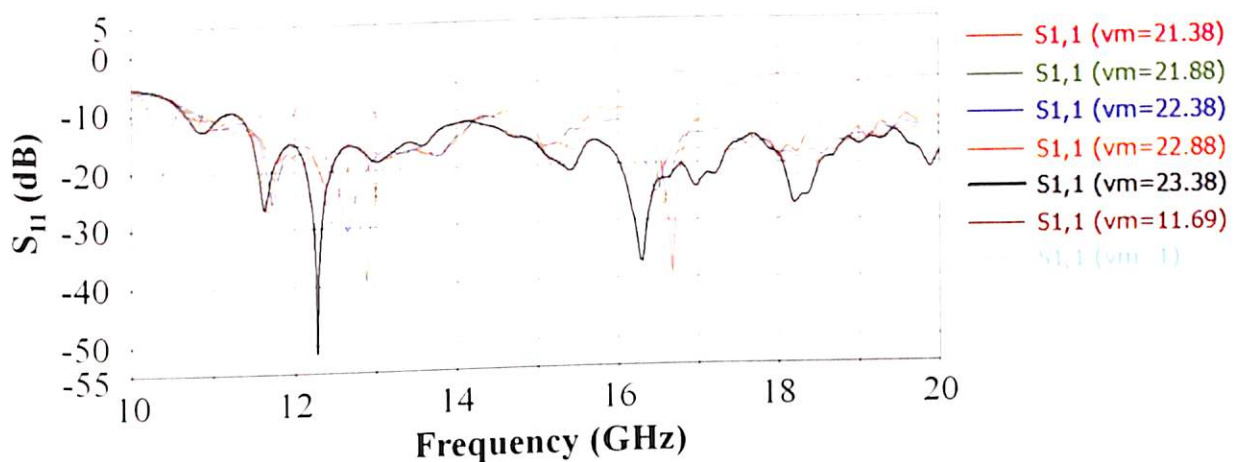
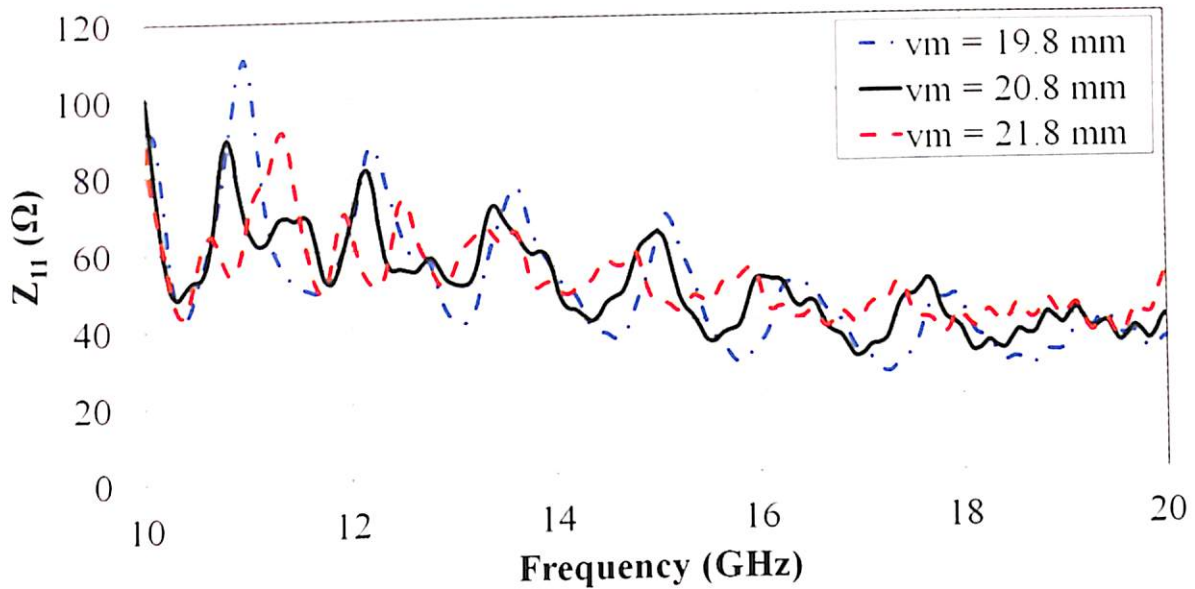


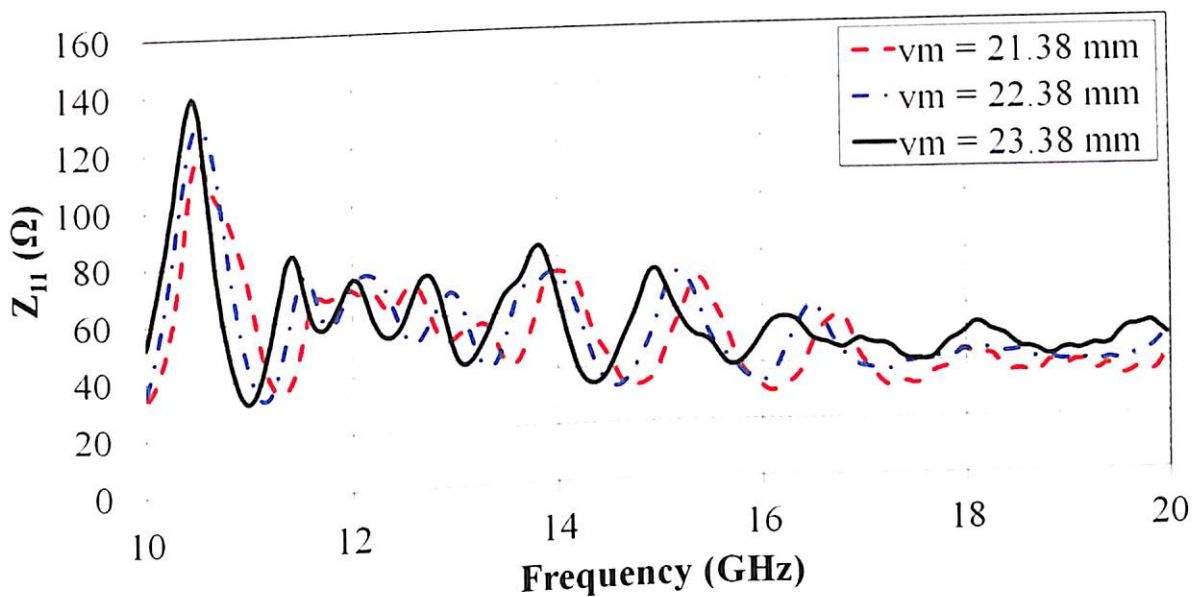
Figure 2.24. Simulated reflection coefficient (in dB) for hexagon to hexagram.

The effect over reflection coefficient  $S_{11}$  can be observed with change in angle or change in coordinate of the interior vertex as it moves towards center of polygon. Pentagonal antenna design is simulated by changing the coordinates of midpoint ( $vm$ ) of edge, from 21.8 to 1 mm on the radial distance in steps of 1 mm from midpoint to center of polygon. Similar simulation is performed on hexagonal patch design, between 23.38 to 1 mm radially. As the angle ( $\theta$ ) decreases with midpoint of edge reaching closer to center of polygon, the multi-resonances disappears from the frequency range i.e. in the operating band. Also frequencies resonating at higher and lower values drifts to  $S_{11}$  values greater than -10 dB as  $\theta$  decreases beyond a certain value. It is observed that, the wideband antenna performance is obtained for

pentagonal and hexagonal patch design respectively. But multiband operation instead of broadband operation is observed at angles lower than  $165.63^\circ$  and  $163.15^\circ$  for pentagonal and hexagonal patch designs respectively. It is observed that the reflection coefficient is below -10 dB for a wideband of 12 to 20 GHz at the optimum vertex coordinates of pentagonal and hexagonal shaped patch as indicated in Figure 2.23 and Figure 2.24 respectively.



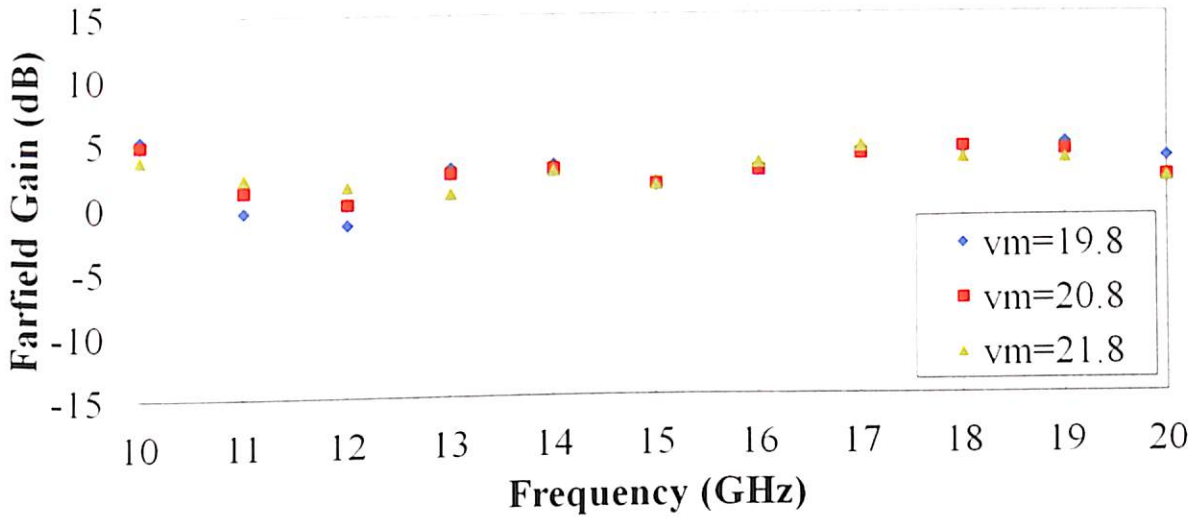
(a) Pentagon to Pentagram



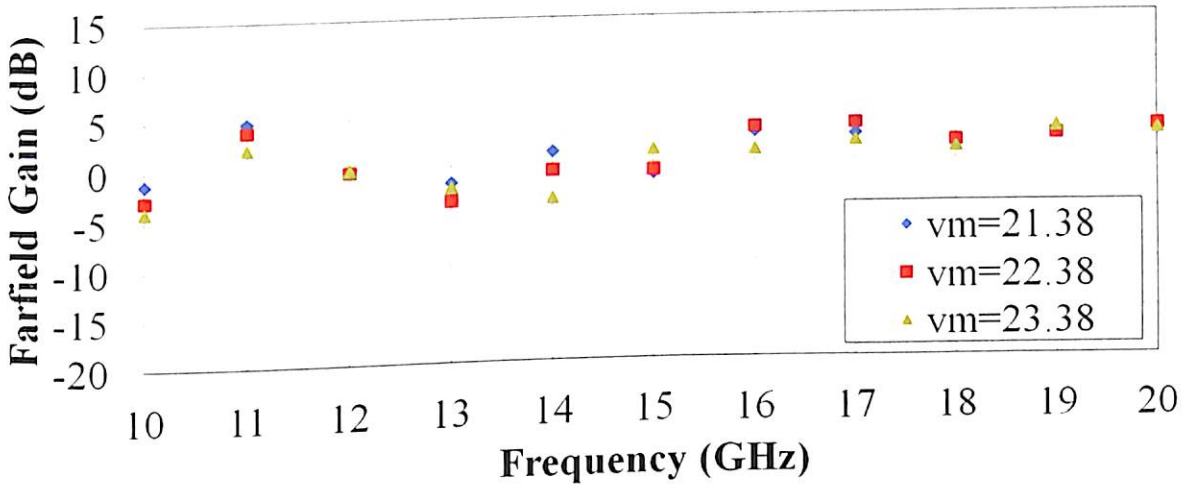
(b) Hexagon to Hexagram

Figure 2.25. Simulated impedance vs. frequency matrix.

Matching impedance to transmission line is one of the significant objectives for a patch and antenna design. The impedance is evaluated for both designs and their variations discussed in earlier and are presented in Figure 2.25(a) and Figure 2.25(b). It is observed that values of  $Z_{11}$  beyond 12 GHz starts stabilizing to approximately  $50 \Omega$  in the operating band for both the polygonal designs and their star geometry variations.



(a) Pentagon to Pentagram

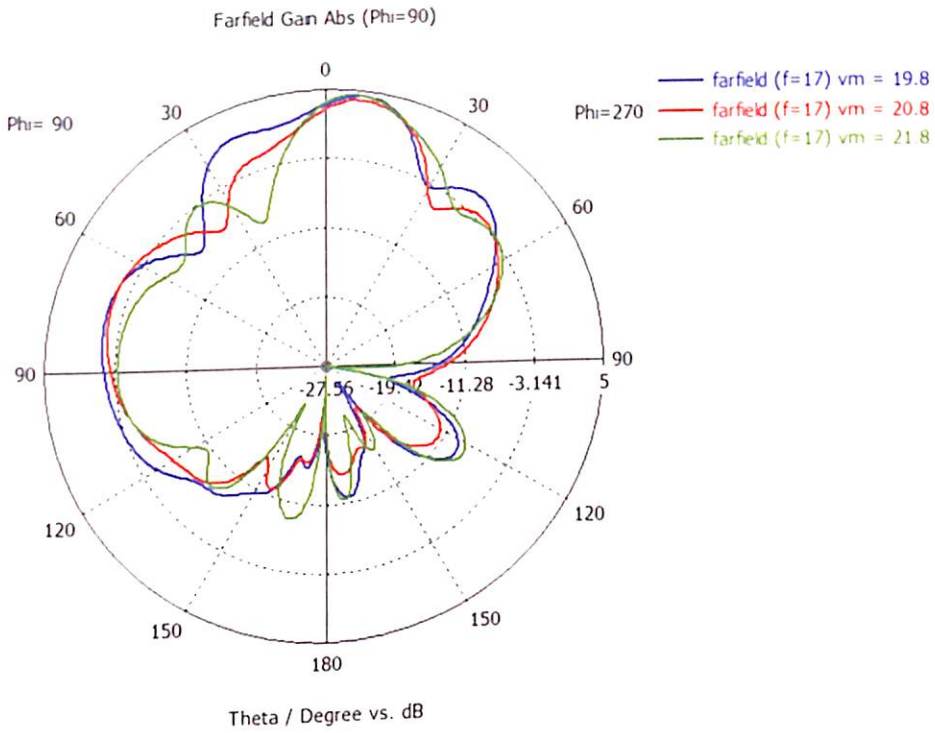


(b) Hexagon to Hexagram

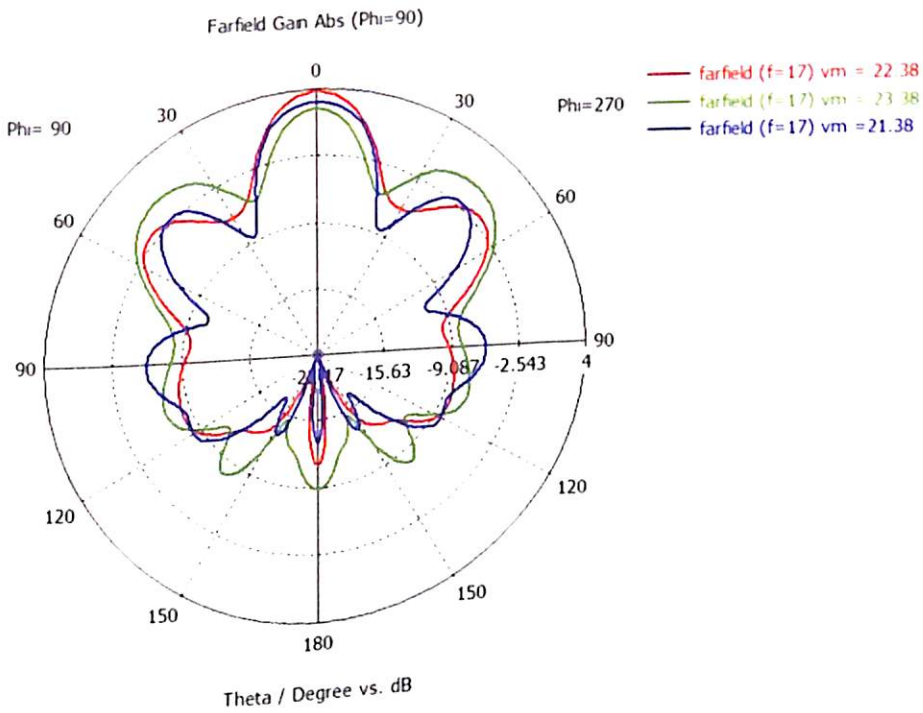
Figure 2.26. Simulated farfield gain vs. frequency.



The effect of the geometry on far field gain (in dB) is evaluated for both polygonal patch designs. The simulated gain response of both polygonal patch antennas is shown in Figure 2.26(a) and Figure 2.26(b).



(a) Pentagon to Pentagram



(b) Hexagon to Hexagram

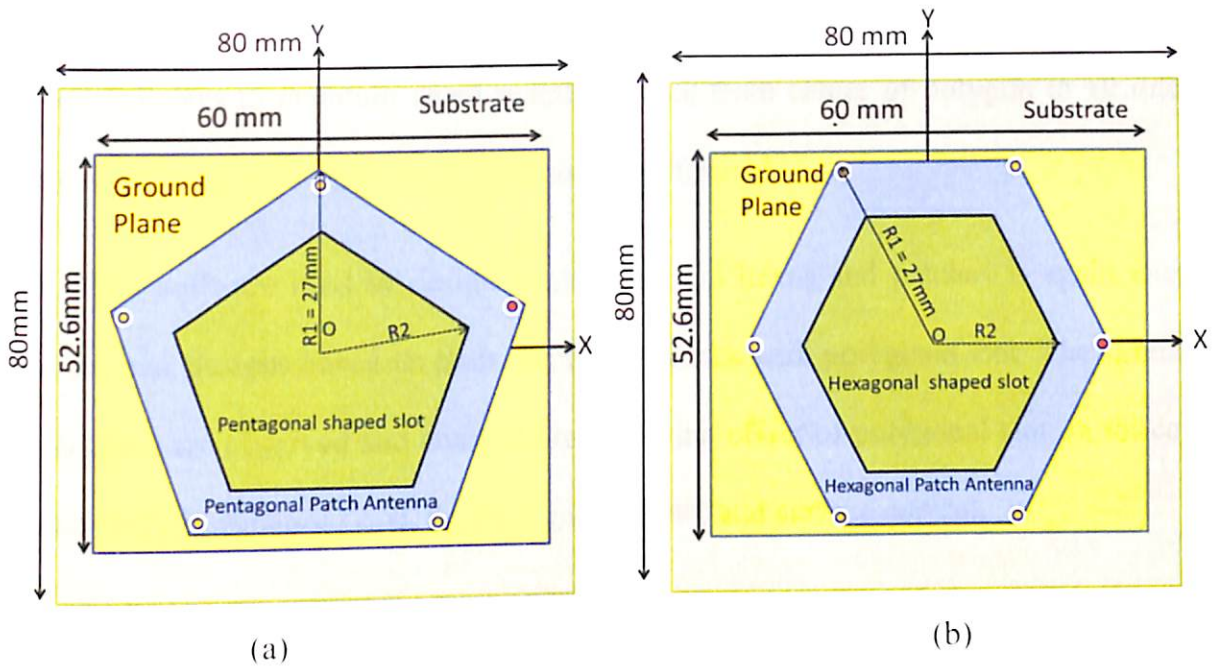
Figure 2.27. Simulated farfield gain at 17 GHz.

Figure 2.26(a) shows that the gain (in dB) in operating band of pentagonal antenna i.e. 12 to 20 GHz reaches to a maximum value of 4.5 dB at 17 GHz. The pentagon patch has a gain greater than 3 dB in the frequency range of 16 to 18 GHz. The pentagram geometries do not provide significant changes in gain, as may be seen in Figure 2.26(a) that gain values for pentagram geometries mostly coincides with gain values for pentagonal patch antenna. In case of hexagonal shaped patch antenna, the gain starts rising above 0 dB after a frequency of 15 GHz and reaches to a maximum value of 2.95 dB at 20 GHz as shown in Figure 2.26(b). But gain values improve at 16 and 17 GHz when patch geometry is modified to hexagram from a hexagon. Satisfactory performance of both polygonal patch geometries is visible at 17 GHz in form of antenna gain and therefore, radiation patterns at 17 GHz for both polygonal patches and their transformations are presented in Figure 2.27(a) and Figure 2.27(b). Radiation patterns suggest that the pentagon and pentagram geometries provide a larger beam width pattern.

## 2.6. Gain Improvement in Polygonal Patch Antennas

In this section the polygonal slot is introduced in polygonal patch in order to enhance the gain at higher frequency. The schematic of a regular pentagonal patch antenna with pentagonal slot at the center is designed in CAD environment provided by CST MWS software as shown in Figure 2.28(a). The antenna in Figure 2.28 is assumed to use a glass epoxy FR-4 substrate ( $\epsilon_r = 4.3$ ,  $\tan \delta = 0.025$ ) of thickness 1.5 mm with an area of  $80 \times 80$  mm<sup>2</sup>. The size of the ground plane is  $60 \times 52.6$  mm<sup>2</sup>.





**Figure 2.28.** Schematic of (a) Pentagonal shaped patch antenna with pentagonal slot (Antenna:A1) (b) Hexagonal shaped patch antenna with hexagonal slot (Antenna:A2).

The pentagonal slot was created by varying radial distance ( $R_2$ ) of pentagonal slot so that the vertices of polygonal slot moves on a trajectory from center of polygon 'O' to radial distance ' $R_2$ ' radially. This results in a pentagonal slot at the center of polygon. The radial distance of pentagonal slot (dashed line in Figure 2.28(a)) are varied from 'O' to ' $R_2$ ' in steps of difference of 1 mm on the radial (dotted) line as shown in Figure 2.28(a), to investigate the effect of pentagonal slot in antenna geometry on antenna's performance. The radial distance of pentagonal slot indicated by a dotted line ' $R_2$ ' in Figure 2.28 is 15 mm for a pentagon with radial distance  $R_1 = 27$  mm.

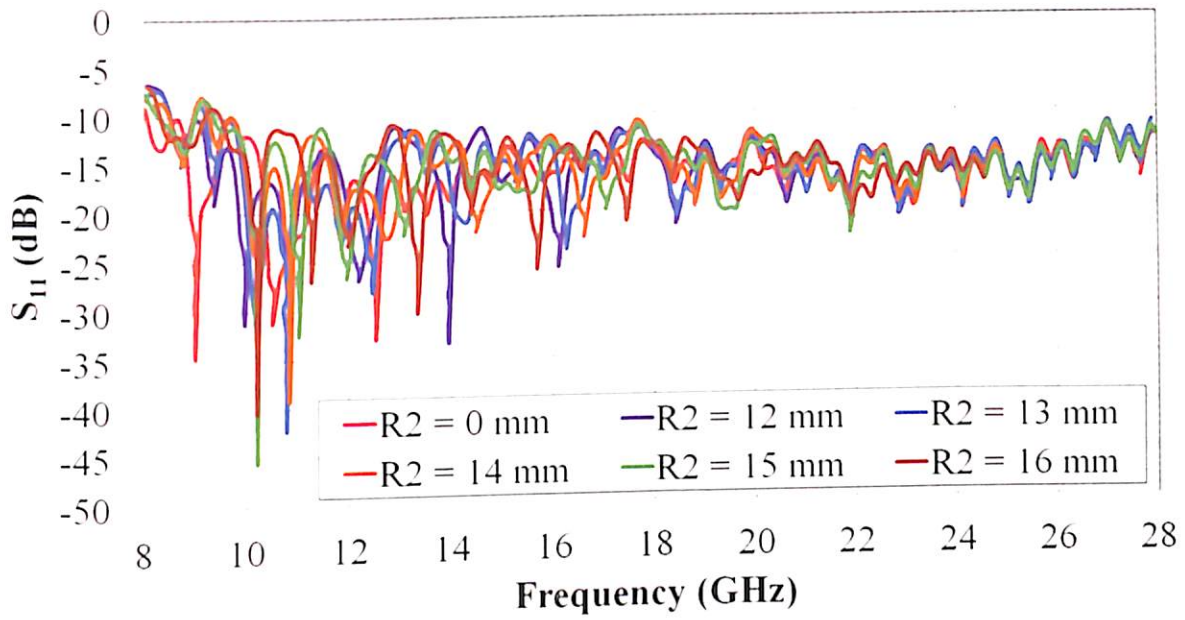
Similar to the schematic of Figure 2.28(a), hexagonal patch is designed with a radial distance of 27 mm from center to its vertex as shown in Figure 2.28(b). The ground plane, substrate material and their dimensions are kept same as for pentagonal patch earlier in section. The feed points are kept at a radial distance of 26 mm from center of hexagon close to its vertices. To analyze the effect of slot on hexagonal patch antenna, the hexagonal slot to its vertices. To analyze the effect of slot on hexagonal patch antenna, the hexagonal slot vertices are moved in steps of 1 mm distance from center of hexagon 'O' toward the radial

distance 'R2' as shown in Figure 2.28(b). The vertices of polygonal slot are defined using variable coordinates to maintain equal radial distance from center of polygon to all interior vertices every time any iteration for simulation is performed.

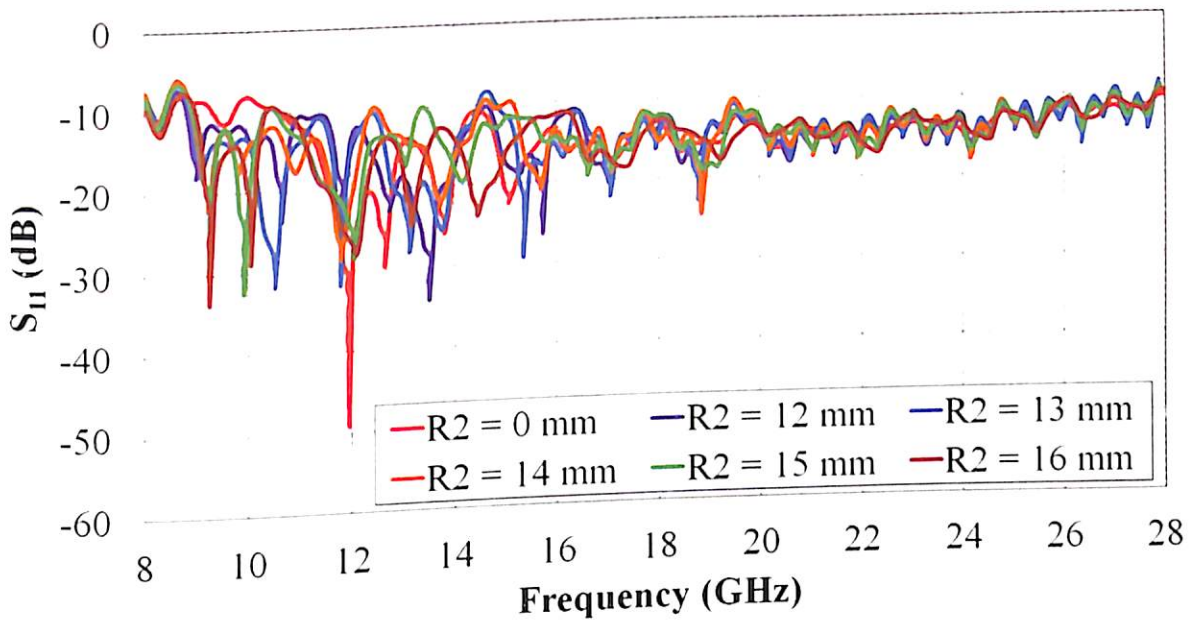
CST MWS software used to design pentagonal and hexagonal patches is again used to simulate antenna designs based on both patch geometries with polygonal slot. The simulated results obtained are observed and analyzed to study the effect of polygonal slot on reflection coefficient ( $S_{11}$ ), impedance ( $Z_{11}$ ), far field gain (in dB) and surface current.

Scattering characteristics of a polygonal antenna is sensitive to polygonal slot as may be seen in Figure 2.29(a) and Figure 2.29(b) for pentagonal and hexagonal patch antennas respectively. The effect over reflection coefficient  $S_{11}$  can be observed with change in radial distance 'R2' or change in coordinate of the vertices of slot as it moves from center of polygon 'O' towards 'R2'. Pentagonal antenna design is simulated by changing the radial distance (R2) of pentagonal slot, from 0 to 26 mm on the radial distance in steps of 1 mm center towards the vertex of polygon. Similar simulation is performed on hexagonal patch design, between 0 to 26 mm radially.

As the radial distance of polygonal slot (R2) increases from center towards vertex of polygon, the multi-resonances disappears from the frequency range i.e. in the operating band. It is observed that, the wideband antenna performance is obtained for pentagonal and hexagonal patch design respectively. But multiband operation instead of broadband operation is observed at R2 lower than 15 and 16 for pentagonal and hexagonal patch designs respectively. It is observed that the reflection coefficient is below -10 dB for a wideband of 12 to 28 GHz at the optimum radial distance of polygonal slot of 'R2' of pentagonal and hexagonal shaped patch as indicated in Figure 2.29(a) and Figure 2.29(b) respectively.



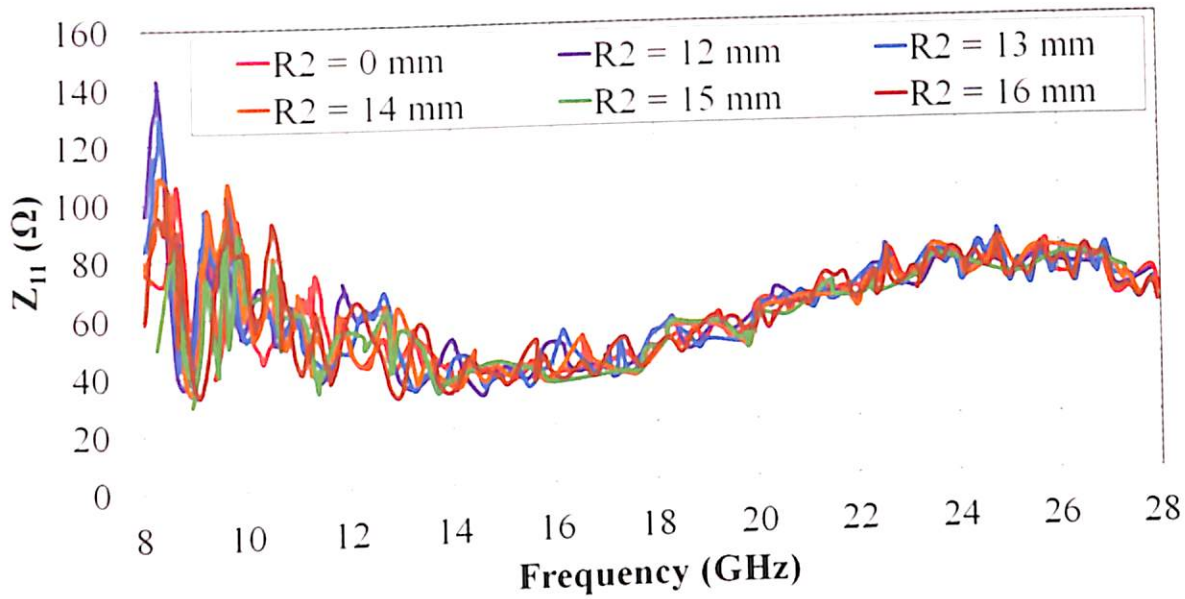
(a) A1



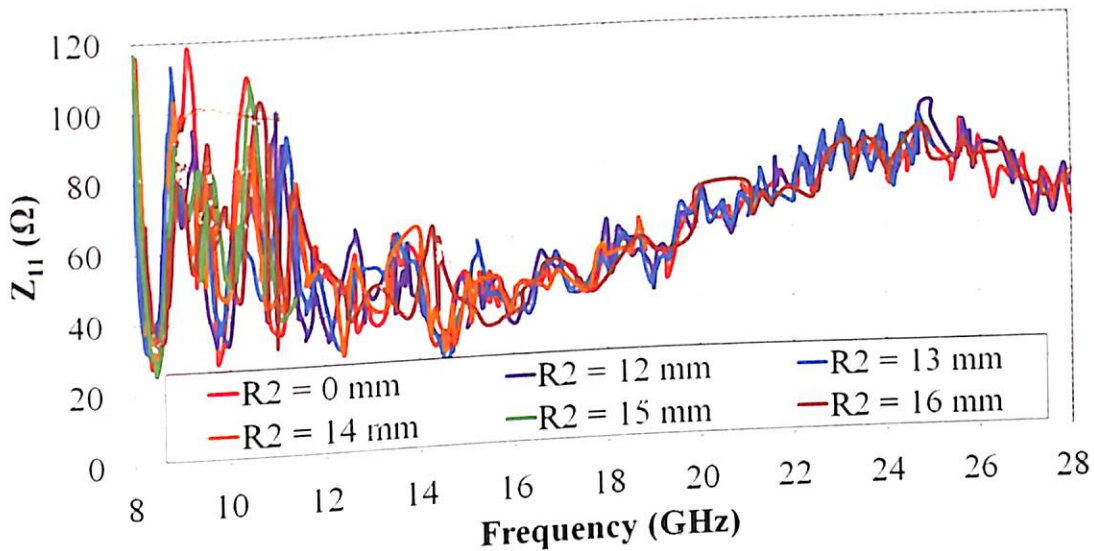
(b) A2

**Figure 2.29.** Simulated reflection coefficient (in dB) for antennas with different values of R2.

The impedance is evaluated for both designs and their variations discussed in earlier and are presented in Figure 2.30(a) and Figure 2.30(b). It is observed that values of  $Z_{11}$  between 18 GHz to 20 GHz is stable to approximately  $50 \Omega$  in the operating band for both the polygonal designs with polygonal slot.



(a) A1



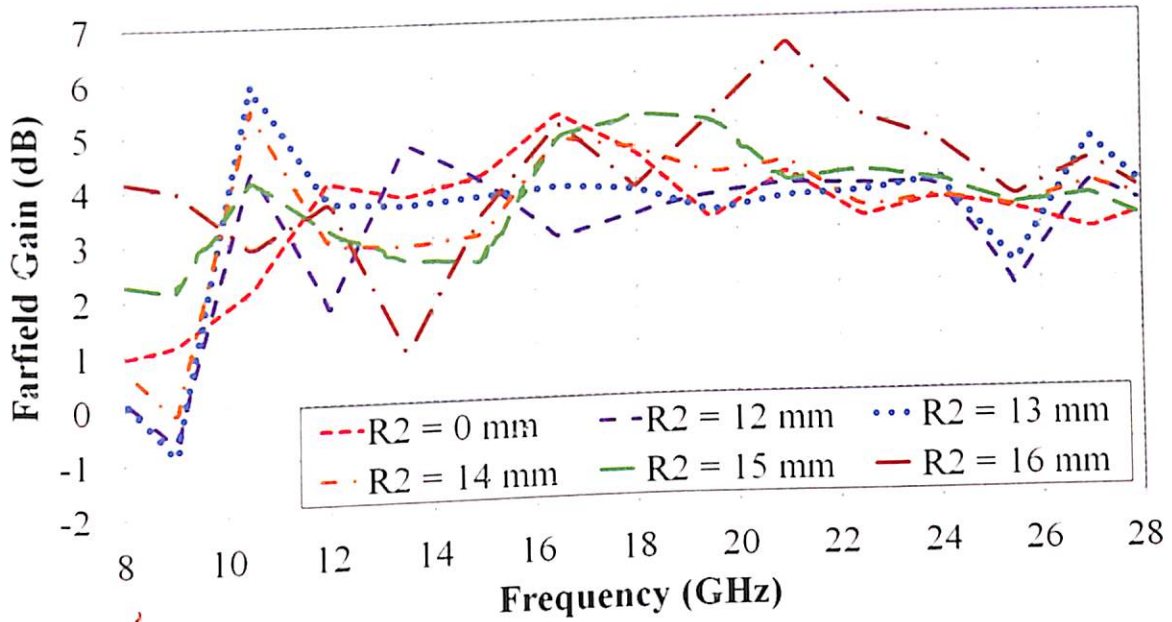
(b) A2

**Figure 2.30.** Simulated impedance vs. frequency matrix for antennas with different values of R2.

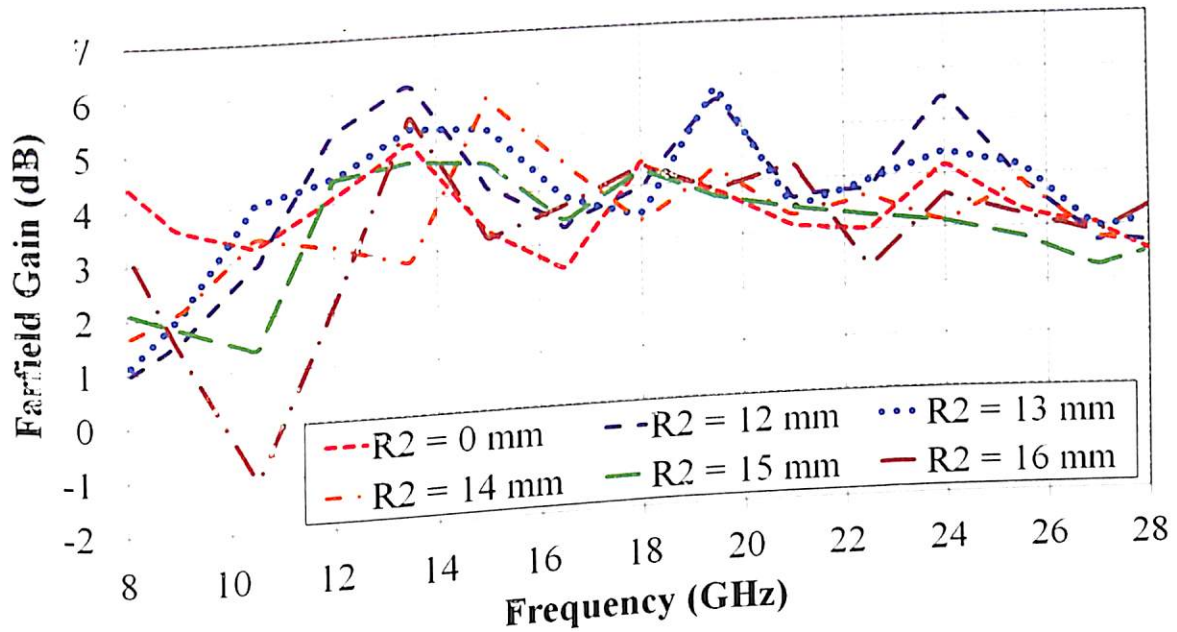
The simulated gain response of both polygonal patch antennas is shown in Figure 2.31(a) and Figure 2.31(b). In Figure 2.31(a) and Figure 2.31(b), the gain points displayed are observed at distant main lobe direction in radiation pattern evaluated at different frequencies for pentagonal and hexagonal patch antennas with polygonal slot with different values of R2 respectively. Figure 2.31(a) shows that the gain (in dB) in operating band of pentagonal antenna with pentagonal slot of radial distance 15 mm i.e. 8 to 28 GHz reaches to a optimum



value of 5.3 dB at 18 GHz. The pentagon patch with pentagonal slot of radial distance 15 mm has a gain greater than 3 dB in the frequency range of 18 to 20 GHz. In case of hexagonal shaped patch antenna with hexagonal slot of radial distance 16 mm has a optimum gain of 4 dB at 18 GHz as shown in Figure 2.31(b).



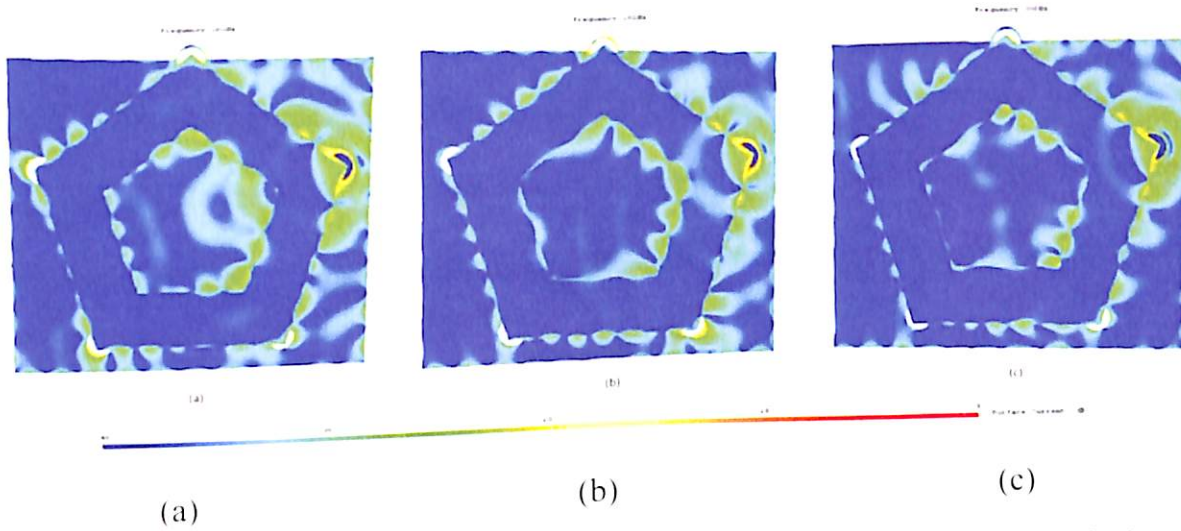
(a) A1



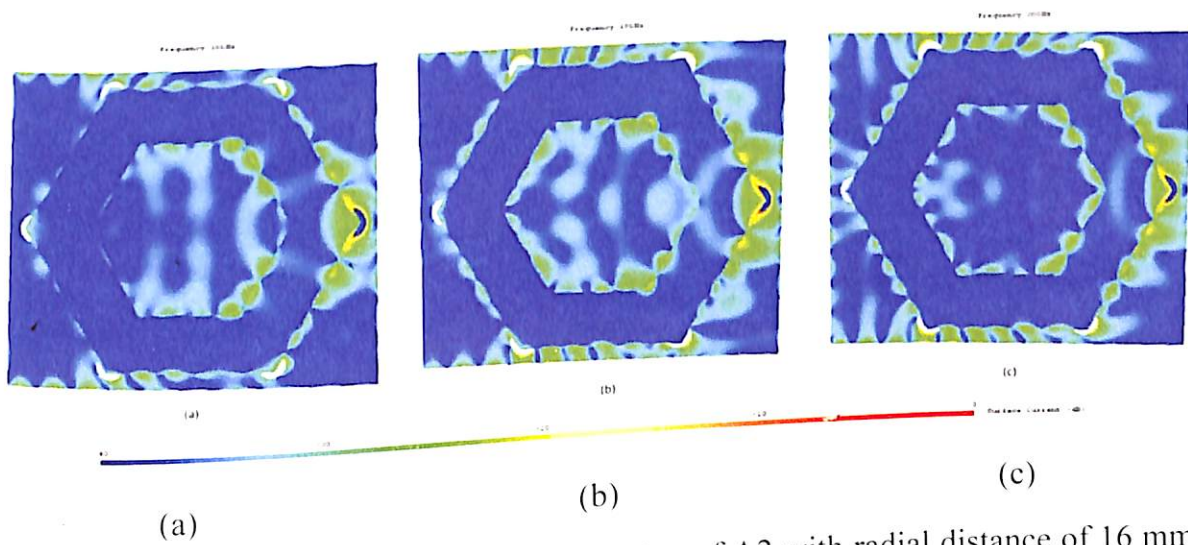
(b) A2

Figure 2.31. Simulated farfield gain vs. frequency for antennas with different values of R2.

The surface-current distributions of both polygonal shaped patch antenna at frequencies 18 GHz, 19 GHz and 20 GHz as shown in Figure 2.32 and Figure 2.33. Pentagon shaped patch antenna with pentagonal slot of 15 mm is taken for analysis of surface current due to improved gain characteristics as shown in Figure 2.32.



**Figure 2.32.** Simulated surface current distribution of A1 with radial distance of 15 mm for the frequency (a) 18 GHz (b) 19 GHz (c) 20 GHz.



**Figure 2.33.** Simulated surface current distribution of A2 with radial distance of 16 mm for the frequency (a) 18 GHz (b) 19 GHz (c) 20 GHz.

Similarly, hexagon shaped patch antenna with hexagonal slot of 16 mm is taken for analysis of surface current as shown in Figure 2.33. At frequencies 18 GHz, 19 GHz and 20 GHz, the surface currents were directed uniformly along all edges of both the polygonal

patches with slight variation at the slot edges. The surface currents that were directed along the patch's edges reduced the antenna's gain towards the lower and higher frequencies of the bandwidth. To understand this current distribution involved in the wideband response surface current at different resonating frequencies i.e. 18 GHz, 19 GHz and 20 GHz are analyzed.

The farfield directivity (in dBi) of both polygonal shaped patch antenna at frequencies 18 GHz, 19 GHz and 20 GHz as shown in Figure 2.34. The hexagonal shaped patch antenna with hexagonal slot of radial distance 16 mm is highly directive as compared to pentagonal shaped patch antenna with pentagonal slot of radial distance 15 mm as shown in Figure 2.34.

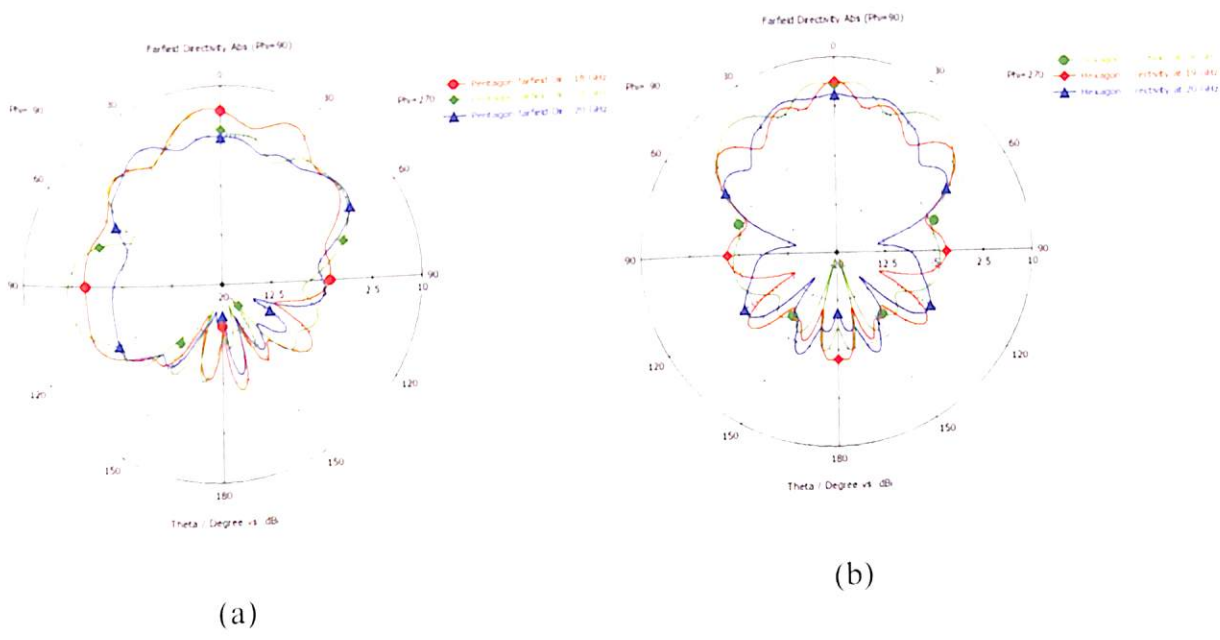


**Figure 2.34.** Simulated farfield directivity at frequencies 18 GHz, 19 GHz and 20 GHz for (a) A1 of 15 mm radial distance (b) A2 of 16 mm radial distance.

## 2.7. Conclusion

In this chapter the fundamental characteristics and performance of probe fed polygonal patch antenna are investigated in detail. Initially, effect of probe position/location is presented. The probe position is varied in order to enhance the bandwidth of antenna and found that vertex is the optimal position for wideband operation of the antenna. The designed antenna probe feed point is varied in order to enhance the bandwidth of antenna. Probe feed analysis suggested



that feed point should be kept closer to vertex of polygon is suitable for a wideband performance of an polygonal patch antenna. The designed antenna bandwidth is 11.4 to 20 GHz. Comparing both pentagonal and hexagonal designs, it was observed that pentagonal patch permits better gain than hexagonal patch over the band of 11.4 to 20 GHz.

It has been demonstrated that different polygonal patch geometry can provide subtle variation in the radiation and impedance characteristics of the patch antenna. The equivalent circuit model and the full wave simulation tool i.e. CST MWS is used to validate the performance of various polygonal geometries. The performance of probe-fed antennas with different patch geometries is compared by varying  $N$  from 3 to 6 with a circular patch designed for L-Band. Triangular patch has comparatively high gain, directivity and efficiency, while hexagonal patch has a lower beam-width that makes it suitable for antenna arrays. Circular and rectangular patches have lower beam-width with poor gain and efficiency compared to hexagonal patch. Polygonal patch antennas required for L-Band applications may be designed by optimizing coordinates of feed point on patch.

The effect of edge perturbation in polygonal patch antenna design is studied. The midpoint of an edge of a polygon is moved towards center of polygon to achieve a polygram or a star geometry. A wideband between 12 to 20 GHz was observed when polygon patch is fed at a vertex of 26 mm from the center of polygon. It is observed that bandwidth, impedance and gain of a pentagonal patch antenna are retained till an angle,  $\theta$ , defined by interior vertex of star geometry is above  $165.63^\circ$ . Similar observations were found with hexagonal patch antenna when  $\theta$  greater than  $163.15^\circ$ . Both angles corresponds to 2 mm distance from center of edge of polygon towards center of polygon. For angles less than  $\theta$ , multiband characteristics are observed and wideband characteristics disappears as return loss greater than -10 dB. Pentagon or pentagram geometries provide a wider bandwidth than hexagon or hexagram geometries. No significant variation is observed in antenna characteristics when

polygons are transformed to polygram geometries, other than a slight improvement in gain of the hexagon patch when transformed to hexagram geometry with  $\theta$  less than  $163.15^\circ$ .

The effect of polygonal slot in polygonal patch antenna design to improve gain characteristics is studied. The pentagon and hexagon shaped patch antenna with pentagonal and hexagonal slot is analyzed respectively. The central polygonal slot is analyzed by varying the radial distance of the slot from 0 to 26 mm. It was observed that pentagon shaped patch antenna with pentagonal slot of 15 mm radial distance improves the gain at 18 GHz. Similarly, hexagon shaped patch antenna with hexagonal slot improves the gain at 18 GHz at a radial distance of hexagonal slot of 16 mm. It is observed that bandwidth, input impedance, farfield gain and surface current of a pentagonal patch antenna are optimum at radial distance of pentagonal slot of 15 mm. Similar observations were found with hexagonal patch antenna with the hexagonal slot of 16 mm. Optimum gain for both the patches is between 18 to 20 GHz.

As it is mentioned earlier, this chapter lays the base of polygonal patch especially, hexagon for the rest of the Thesis. It is very significant to understand the basic character of hexagon because many issues and concepts of the probe fed hexagon antenna will be utilized and exploited in the subsequent chapters of the Thesis.